

Topological screening and interference of fractionally charged quasi-particles

Ivan P. Levkivskyi^{1,2}, Jürg Fröhlich³ and Eugene V. Sukhorukov¹

¹*Département de Physique Théorique, Université de Genève, CH-1211 Genève 4, Switzerland*

²*Physics Department, Kyiv National University, 03022 Kyiv, Ukraine and*

³*Institute of Theoretical Physics, ETH Hönggerberg, CH-8093 Zurich, Switzerland*

Interference of fractionally charged quasi-particles is expected to lead to Aharonov-Bohm oscillations with periods larger than the flux quantum Φ_0 . However, according to the Byers-Yang theorem, observables of an electronic system are invariant under adiabatic insertion of a quantum of singular flux. We resolve this seeming paradox by considering a *microscopic* model of an electronic Mach-Zehnder interferometer made from a quantum Hall liquid at filling factor $\nu = 1/m$. Such interferometers have the shape of a Corbino disk and utilize quantum Hall edge states in place of optical beams and quantum point contacts as beam splitters connecting different edge channels. An approximate ground state of such an interferometer is described by a Laughlin type wave function, and low-energy excitations are incompressible deformations of this state. We construct a low-energy effective theory by projecting the state space of the liquid onto the space of such incompressible deformations and show that the theory of the quantum Hall edge so obtained is a generalization of a chiral conformal field theory. Amplitudes of quasi-particle tunneling in this theory are found to be insensitive to the magnetic flux threading through the hole in the Corbino disk. This behavior is a consequence of *topological screening* of the singular flux by the quantum Hall liquid. We describe strong coupling of the edges of the liquid to Ohmic contacts and the resulting quasi-particle current through the interferometer with the help of a master equation. As a function of the singular magnetic flux, the current oscillates with the electronic period Φ_0 , i.e., our theory conforms to the Byers-Yang theorem. These oscillations, which originate from the Coulomb blockade effect, are suppressed with increasing system size. In contrast, when the magnetic flux through the interferometer is varied with a modulation gate, current oscillations have the quasi-particle period $m\Phi_0$ and survive in the thermodynamic limit.

PACS numbers: 73.23.-b, 73.43.-f, 85.35.Ds

I. INTRODUCTION.

Since its discovery, in 1980, the quantum Hall (QH) effect¹ has been a very rich source of interesting problems related to topological and correlation effects in condensed matter systems. The QH effect is observed in two-dimensional electron gases² (2DEG) exposed to a strong magnetic field perpendicular to the plane of the gas. At appropriate electron densities, the 2DEG forms an incompressible liquid. The QH effect manifests itself in the precise and universal quantization of the Hall conductance. This behavior originates from an interplay between the Landau quantization of the orbital motion of electrons³ and interaction effects, which leads to the formation of a bulk energy gap. As a consequence an incompressible state is formed in the bulk of the 2DEG. At the edge of a 2DEG exhibiting the QH effect there exist, however, gapless chiral modes that are the quantum analogue of classical skipping orbits.⁴ In the presence of strong Coulomb interactions, these modes can be viewed as collective edge plasmon modes. Remarkably, it has been predicted^{5,6} that, at fractional fillings of the Landau levels, besides the collective modes the edge states of the 2DEG also describe quasi-particles with *fractional charges* and fractional statistics.⁷ For instance, in QH liquids with filling factor $\nu = 1/m$, where m is an odd integer, Laughlin quasi-particle excitations have an electric charge $e^* = e/m$, where e is the elementary electric charge. Such excitations can be scattered between oppo-

site edges at narrow constrictions forming quantum point contacts (QPC), thus contributing to a backscattering current.

The fractional charge of Laughlin quasi-particles has been confirmed, experimentally, in measurements of the shot noise of weak backscattering currents.⁸ The quasi-particle charge in these experiments is inferred from the Fano factor of noise, which is the ratio of the noise power to the average backscattering current. Although, at present, there is a consensus on the interpretation of the experimental results, this type of measurement does not, in general, represent a direct test of the fractional charge of quasi-particles.⁹ Indeed, the Fano factor of noise is not universal and may be reduced or enhanced for various reasons.¹⁰ For instance, the so called “charge fractionalization” in nonchiral one-dimensional systems^{11,12} is a property of collective modes that has nothing to do with the existence of fractionally charged quasi-particles. Nevertheless, this phenomenon reduces the Fano factor of noise at relatively high frequencies.¹³

A direct measurement of the quasi-particle charge should rely on its definition as a coupling constant in the interaction Hamiltonian coupling matter to the electromagnetic field and on the quantum nature of quasi-particles. The most appealing approach is to make use of the Aharonov-Bohm (AB) effect,¹⁴ which relies on the fact that the interference of quasi-particles is affected by a magnetic flux. Following a commonly used formulation of this effect, we consider a gedanken interference

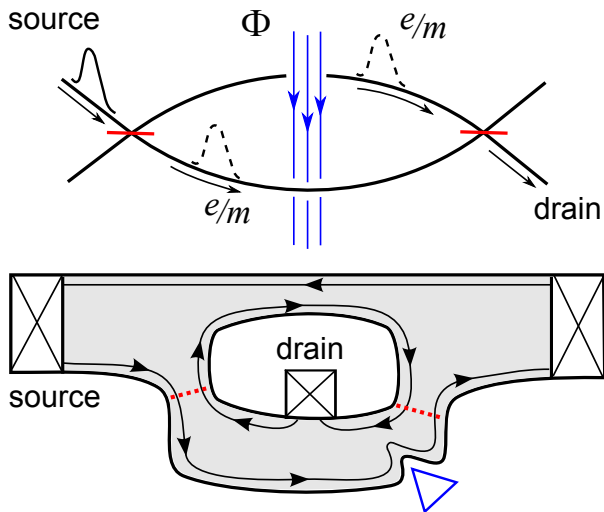


FIG. 1: An electronic analogue of an optical Mach-Zehnder (MZ) interferometer is shown schematically. *Upper panel:* According to a gedanken formulation of the Aharonov-Bohm effect, quasi-particles with fractional charge e/m propagate from a source to a drain via two beam splitters, and enclose a singular magnetic flux Φ . *Lower panel:* Schematic sketch of a typical experimental realization of the MZ interferometer in a quantum Hall system.^{20–24} Chiral edge states, shown by arrows, play the role of optical beams. They are split at two quantum point contacts indicated by dashed lines. The source and drain are Ohmic contacts. The quantum Hall liquid is confined to a region with the topology of a Corbino disk (indicated by gray shading). The magnetic flux through the interferometer is typically changed by a modulation gate, shown as a blue triangle. However, it is possible, at least in principle, to insert a singular magnetic flux through the hole in the Corbino disk.

experiment shown in the upper panel of Fig. 1. Quasi-particles of charge e/m traverse two beam splitters and follow paths that enclose a *singular* magnetic flux Φ . The relative phase between the two amplitudes, for the upper and lower path, is shifted by an amount of $2\pi\Phi/m\Phi_0$, which leads to AB oscillations in the current from the source to the drain as a function of the flux Φ with quasi-particle period $m\Phi_0$. The quasi-particles can then be detected by differentiating their contribution to the AB effect from electron oscillations with period Φ_0 .

AB oscillations with quasi-particle periods larger than the flux quantum have been observed in a number of recent experiments^{15–17} involving QH interferometers of the Fabry-Pérot type. In these interferometers, chiral edge states of a QH system form a loop. The magnetic flux through the loop is varied either by changing the strength of the homogeneous magnetic field, or by deforming the edge of the QH system with the help of a modulation gate. The theoretical interpretation of the experimental results as demonstrating a quasi-particle AB effect appears obvious. Nevertheless, it remains the subject of a theoretical debate for the following reasons. First of all, oscillations of the current through a Fabry-Pérot interferometer as a function of the magnetic flux

could originate from the Coulomb blockade¹⁸ rather than from interference effects. Second, the original gedanken formulation of the AB effect outlined above requires a singular magnetic flux threading through the region of the plane not accessible to quasi-particles. This is not the case in the experiments, see Ref. [15–17], where quasi-particles are directly affected by the magnetic field. Third, and more importantly, the gedanken formulation of the AB effect itself leads to a paradox: In any electronic system, including fractional QH systems, AB oscillations should have an electronic period Φ_0 , according to the Byers-Yang theorem.¹⁹ This is so, because, after adiabatic insertion of a flux quantum through a hole in the sample, an electronic system relaxes to its initial state, since the flux quantum can be removed by a single-valued gauge transformation.

The first two problems can in principle be solved by using a QH interferometer of a different type, namely the electronic analog of an optical Mach-Zehnder (MZ) interferometer.²⁰ Very recently, AB oscillations in these interferometers utilizing QH liquids at integer filling factors have become the subject of intensive experimental studies^{20–24} and theoretical discussions.^{25–30} A typical electronic MZ interferometer is sketched, schematically, in the lower panel of Fig. 1. In this interferometer the 2DEG is confined to a region with a shape topologically equivalent to an annulus, i.e., a so called Corbino disk. Chiral edge states are used in place of optical beams and two QPCs (shown by dashed lines) play the role of optical beam splitters. Ohmic contacts are attached to the inner and outer edge of the Corbino disk and serve as a source and drain for the current. Although MZ interferometers are more difficult to manufacture, they have an advantage over Fabry-Pérot interferometers: First, modes in two edge channels of the interferometer propagate in the same direction and without backscattering, because they are interrupted by Ohmic contacts. As a result, the Coulomb blockade can be avoided in these systems by strongly coupling the edge states to Ohmic contacts. Second, a singular magnetic flux can, at least in principle, be inserted in the hole of the Corbino disk, i.e., in the region not accessible to electrons. Therefore, electronic MZ interferometers might be thought to be a solid-state implementations of the gedanken experiment shown in the upper panel of Fig. 1. They may thus represent an ideal system for addressing the third problem mentioned above, namely the paradox associated with the Byers-Yang theorem.

There have been several theoretical attempts to resolve this paradox.^{31–36} In early work [31], Thouless and Gefen have considered the energy spectrum of a QH liquid confined to a Corbino disk and weakly coupled to Ohmic contacts. They have found that as a result of weak quasi-particle tunneling between the inner and the outer edge of the Corbino disk, the energy spectrum, and consequently, “any truly thermodynamic quantity” is a periodic function of the magnetic flux with the electronic period Φ_0 . Although Thouless and Gefen have made an

important first step towards understanding the AB effect in QH interferometers, their analysis is rather qualitative, and some of their statements concerning the tunneling rates and currents are not firmly justified.³⁷ The results of their work are difficult to interpret at the level of effective theories. But, more importantly, they cannot easily be generalized to the situation where the magnetic flux is varied with the help of a gate voltage. This situation has stimulated further interest in the fractional AB effect in MZ interferometers.

More recently, a number of authors (see Refs. [32–34]) have proposed that the correct description of the MZ interferometers should take into account the presence of additional quantum numbers in a QH state. In the thermodynamic limit, averaging the quasi-particle current over these quantum numbers is claimed to restore the electronic AB periodicity. These quantum numbers are usually introduced ad hoc, with minimal justification. Depending on the particular theoretical discussion, they are represented either in terms of so called Klein factors in the tunneling operators,³⁸ or as additional phase shifts induced by quasi-particles localized at the inner edge of the Corbino disk.³³ We are aware of only one attempt to theoretically justify the introduction of Klein factors in MZ interferometers: In their recent work [35], Ponomarenko and Averin implement a resummation of electron tunneling processes between the inner and outer edge and claim that there is a duality to weak quasi-particle tunneling, where the Klein factors arise naturally. However, their analysis is done entirely at the level of an effective theory, where weak quasi-particle and weak electron tunneling are the two fixed points of a renormalization group flow. There is no guarantee that microscopic considerations will yield the same result.

The results of the works [32–35] can be summarized as follows: They resolve the Byers-Yang paradox by stating that AB oscillations with quasi-particle periods cannot be observed in the steady-state current through an MZ interferometer. In other words, these works do not discriminate between the effects of a singular flux, modulation gate, and a homogeneous magnetic field. Our findings do not agree with this conclusion. In previous work,³⁶ we have argued that quasi-particle AB oscillations should be observable if the magnetic flux is varied by deforming the edge of the QH system, or, alternatively, by changing the strength of the homogeneous magnetic field. We have proposed to use this effect as a spectroscopic tool for experimental investigations of scaling dimensions of quasi-particles at different filling factors. In the present paper we construct the theoretical basis for this effect. Our predictions can be verified experimentally by pinching off the QPCs and comparing the regimes of weak electron tunneling and of weak quasi-particle tunneling, where the periods of AB oscillations should differ from each other by a factor of m . Our theoretical arguments are presented on three different levels: By considering a microscopic wave function for the ground state of an MZ interferometer, deriving an effective theory from it,

and describing the relaxation of the interferometer to a stationary state with a master equation.

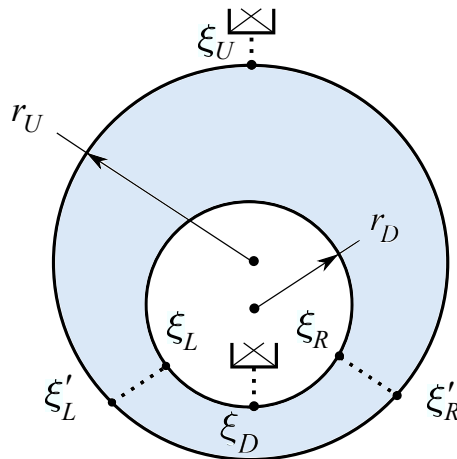


FIG. 2: Illustration of our model of a Mach-Zehnder interferometer. The 2DEG in the QH effect regime is confined to a region, shown by grey shadow, which is an asymmetric Corbino disk. The inner and outer edge of the 2DEG are circles of radii r_D and r_U , respectively. At the points ξ_U and ξ_D the Corbino disk is connected to Ohmic reservoirs. The quasi-particle tunneling between the inner and the outer edge takes place at two QPCs, shown by dashed lines, that connect the points ξ_ℓ and ξ'_ℓ , with $\ell = L, R$.

At the level of the microscopic theory we arrive at the rather surprising conclusion that the AB effect, in its original formulation,¹⁴ is not exhibited by QH interferometers. In order to clarify this important claim, we first remark that the original formulation of the effect relies on a single-particle picture, where a particle wave travels through the interferometer, as shown in the upper panel of Fig. 1. While traveling through the upper and lower paths of the interferometer, the particle wave accumulates a phase difference containing three contributions: a dynamical and a kinematic one, and the AB phase differences. This picture is quite appealing and is therefore commonly used in the physics literature. However, for the description of the AB effect, this picture is redundant, because at low energies, the dynamical phase can be neglected. Instead, it is more appropriate to consider the relative phase of the wave function overlaps at the two beam splitters. Moreover, in correlated systems, such as QH interferometers, the single-particle description is, strictly speaking, not applicable. In particular, the naive (gedanken) formulation of the AB effect may lead to serious misconceptions and problems, one of them being the Byers-Yang paradox; (see also the discussion in Sec. VI).

Thus, we propose to investigate many-particle wave function overlaps. To this end, we consider a microscopic model of an MZ interferometer schematically shown in Fig. 2. A QH liquid at filling factor $\nu = 1/m$ is confined to a region between two circles of radii r_U and r_D . By separating the centers of the two circles, we deliberately break the axial symmetry in order to avoid specific

geometry effects and to exhibit the general character of our results. The inner and outer edges of the QH liquid are connected to Ohmic contacts at points ξ_U and ξ_D via strong electronic tunneling. Weak backscattering at two QPCs is modeled by quasi-particle tunneling between points ξ_L , ξ'_L , and ξ_R , ξ'_R , as indicated in Fig. 2 by dashed lines. The state of the QH liquid is described by a Laughlin-type wave function, see Eqs. (1) and (2). We generalize the Laughlin wave function, in order to take into account the deformation of the QH edge caused by the modulation gate, Eq. (5). Exactly the same procedure can be applied in order to describe a QH liquid of arbitrary shape. This will allow us to choose $\xi_L \simeq \xi'_L$ and $\xi_R \simeq \xi'_R$ in order to describe realistic QPCs. Finally, the effect of a singular flux threading through the hole in the interferometer is described by the wave function in Eq. (6).

It turns out that the wave function overlap (38) at a point ξ , i.e., the matrix element of a quasi-particle tunneling operator (37), is a single-valued function of ξ , for any number, M , of quasi-particles in the interferometer. This implies that the commonly used picture,³⁹ according to which every quasi-particle carries a “statistical phase tube” seen by other quasi-particles as an additional phase shift, does not apply *naively* to MZ interferometers. More importantly, in the presence of a singular magnetic flux Φ , the Laughlin wave function (6) contains a flux-dependent factor, which depends *only on the distance* between electrons and the flux tube. In other words, the AB phase from the gauge field is canceled, locally, by the phase induced by the physical deformation of the Laughlin wave function in response to the singular flux. This fact is independent of the shape of the QH system and leads to an exact cancellation of the relative AB phase in the tunneling amplitudes (55). Thus, we arrive at the rather remarkable result that the AB effect, in its original formulation,¹⁴ does not exist in QH interferometers. However, in response to local edge deformations induced by a modulation gate, as described by Eq. (5), the wave function and, consequently, the tunneling amplitudes acquire a relative phase proportional to the total change in the homogeneous magnetic flux through the QH liquid enclosed by the interferometer. This effect leads to oscillations in the current with quasi-particle period $m\Phi_0$. Note that this phenomenon, which we propose to call a *quasi-particle AB effect*, does *not* violate the Byers-Yang theorem.

In order to connect these findings to the low-energy effective theory of the QH effect,^{5,6} we consider small incompressible deformations of the ground state of an MZ interferometer, as shown in Fig. 3, below. The microscopic wave function resulting from such deformations, given by Eqs. (3) and (4), is parameterized by an infinite set of variables, t_k . We invoke the classical plasma analogy⁷ and follow the steps of Ref. [40] in order to project the microscopic Hamiltonian onto the subspace of these deformations. After the projection, the variables t_k turn into oscillator operators, a_k , with canonical com-

mutation relations (25). These operators describe *gapless* plasmon excitations at the edge of the QH liquid. The projected Hamiltonian (35) contains the oscillator part with a linear spectrum and the Coulomb charging energy, which depends on the number of quasi-particles, M , and the number of electrons, N , in the QH system. The projected tunneling operators take the form of vertex operators (43). Interestingly, we do not find any trace of Klein factors³⁸ in the tunneling amplitudes. Moreover, contrary to earlier suggestions,³² the tunneling Hamiltonians at different points in space do not commute with each other (see Appendix A). We show that the low-energy theory so derived agrees well with the effective theory of Wen and one of us,^{5,6} generalized so as to take into account the finite size of the QH system and the effects of a modulation gate and of a singular magnetic flux.

At the level of the effective theory, the three contributions to the overall phase shift in the current oscillations, the dynamical, kinematic, and AB phase mentioned above, acquire the following interpretation.^{29,36} The dynamical phase has its origin in temporal fluctuations of the charge density at the edge described with the help of the oscillator operators, a_k . These fluctuations suppress the AB effect at high temperatures but can be neglected at low energies. The kinematic phase can be viewed as a contribution of zero modes. In order to interpret the AB phase, we note that the effective theory in Refs. [5] and [6] arises as a boundary contribution to a topological Chern-Simons theory⁴¹ describing the bulk of the 2DEG in the presence of an external electromagnetic field. Within this theory, the AB phase is picked up by a Wilson loop [see Eq. (73)] along the interferometer contour. There are two contributions to this phase: one is proportional to the gauge field describing the singular magnetic flux; the other one comes from the charge accumulated at the inner edge as a result of an adiabatic variation of the singular flux. It turns out that these two contributions cancel each other exactly, so that the total phase due to a singular magnetic flux vanishes. In the particular gauge we use, the cancellation is local in space and can be viewed as screening of the singular flux by the QH liquid. We propose to call this effect *topological screening*, in order to emphasize its independence of the particular sample geometry.

Having constructed the low-energy theory of an isolated QH system, we proceed to analyze the quasi-particle transport at QPCs and the electron transport at Ohmic contacts. We apply the tunneling approximation to describe both processes as rare transitions that change the numbers, N_D and N_U , of electrons at the inner and outer edge of the Corbino disk and the number, l , of quasi-particles at the inner edge, where $l = 0, \dots, m-1$. The dynamics of the MZ interferometer on a long time scale is described by a master equation for the probability to find the system in a state corresponding to given values of (N_D, N_U, l) . In order to model Ohmic contacts, we consider the limit of strong electron tunnel-

ing. As a result, the density matrix in the electronic sector approaches the product of two equilibrium distributions determined by the Ohmic reservoirs (78). Then we sum over the electronic numbers N_D and N_U and obtain the master equation, see (80) and (81), for the density matrix in the quasi-particle sector indexed by l . Finally, solving this master equation, we find the current through the MZ interferometer as a function of the magnetic flux, thereby establishing the *main results* of our paper. Namely, we find that the current oscillates as a function of the singular magnetic flux with the electronic period Φ_0 , and these oscillations are exponentially suppressed with temperature and system size. This implies that they can be viewed as a Coulomb blockade effect. In contrast, as a function of the magnetic flux modulation due to a gate, the current oscillates with the quasi-particle period $m\Phi_0$, and these oscillations survive in the thermodynamic limit. Thereby, the Byers-Yang paradox is resolved.

An important result of our analysis is to predict the screening of the magnetic flux through the hole in a Corbino disk by the QH liquid. Since this effect has a topological character, i.e., does not depend on the distribution of the flux inside the hole and the sample geometry, our prediction also holds in a homogeneous magnetic field. Thus, the effect of topological screening can be tested, in principle, in an experiment with an MZ interferometer by changing the area of the hole with a modulation gate but preserving the area of the QH liquid inside the interferometer, as shown in Fig. 9. We predict that, after the application of a gate voltage, the periodicity of the current as a function of the homogeneous magnetic field will not change, contrary to a naive expectation that the period depends on the total area of the interferometer. This is because the flux through the hole is screened and the AB phase is proportional to the area of the 2DEG enclosed by the interferometer paths. The last fact leads also to another important prediction: in a strongly disordered system stuck on a QH plateau, the topological screening leads to a linear dependence of the AB period (measured in AB oscillations, as a function of the homogeneous magnetic field) on the filling factor. This is because by changing the filling factor we also change the area of the QH liquid inside the interferometer, even if the interfering paths are fixed. We stress that our predictions also apply to a QH system at the $\nu = 1$ plateau, where the measurements can be done more easily (see also the discussion in Sec. VI).

Our paper is organized as follows. In Sec. II we construct the ground state wave function of an MZ interferometer in the fractional QH effect regime and discuss the effects of a singular magnetic flux and of a modulation gate. In Sec. III, by projecting the microscopic Hamiltonian and tunneling operators onto the subspace of states corresponding to small incompressible deformations of a QH liquid, we derive the low-energy theory of the MZ interferometer. Then, in Sec. IV, we compare the description derived from our microscopic theory with

the one provided by the effective Chern-Simons theory. In Sec. V we use the low-energy effective Hamiltonian in order to find the density matrix of the MZ interferometer strongly coupled to Ohmic reservoirs and to evaluate the charge current in the presence of a singular magnetic flux and of a modulation gate. We then discuss physical consequences of topological screening and propose simple experiments to test our predictions in Sec. VI. Finally, in Appendix A, we discuss the commutation relations for the quasi-particle operators and for tunneling operators, which are important ingredients of our theory.

II. MICROSCOPIC DESCRIPTION OF THE MZ INTERFEROMETER

In this section we construct the many-particle wave functions of the ground state and of gapless excited states of an MZ interferometer. We do this step by step, starting from the Laughlin wave function and manipulating it, in order to arrive at a realistic model of the interferometer. We first present the most important results before we prove them, in Sec. II A, using the classical plasma analogy.⁷ The variational wave function, proposed by Laughlin in Ref. [7] and later justified by Haldane and Rezayi in Ref. [42], describes an approximate ground state, $|N\rangle$, of a QH system with N electrons at filling factor $\nu = 1/m$:

$$\langle \underline{z} | N \rangle = \prod_{i < j}^N (z_i - z_j)^m \exp \left(- \sum_i^N \frac{|z_i|^2}{4l_B^2} \right). \quad (1)$$

Here \underline{z} denotes a set of complex coordinates $z_i = x_i + iy_i$ describing the position of the i^{th} electron, $i = 1 \dots N$, and $l_B = \sqrt{\hbar c / eB}$ is the magnetic length. It is known⁴ that the wave function (1) describes a circular droplet of a QH liquid of constant density $\rho_{\text{bg}} = 1/(2\pi m l_B^2)$ and of radius $r = l_B \sqrt{2mN}$.

In the next step, we add to the state (1) a macroscopic number, M , of Laughlin quasi-particles⁷ at the point z_0 :

$$\langle \underline{z} | N, M \rangle = \prod_i^N (z_i - z_0)^M \langle \underline{z} | N \rangle. \quad (2)$$

In Sec. II A we explicitly show that the wave function (2) describes a QH state of constant electron density ρ_{bg} inside a Corbino disk, as shown in Fig. 2. The inner hole of the disk is centered at z_0 and has a radius $r_D = l_B \sqrt{2M}$, while the outer radius of the disk is given by $r_U = l_B \sqrt{2(M + mN)}$. We stress that the sample geometry so obtained is not symmetric under rotations around the axis through the origin perpendicular to the sample plane, for $z_0 \neq 0$. We deliberately break the axial symmetry in order to avoid accidental effects of symmetry and to come closer to a realistic model of an interferometer (see Fig. 1, lower panel).

Additional small incompressible deformations of the QH liquid disk may be described as follows. We note

that all states of the lowest Landau level can be described by holomorphic functions of electron coordinates. We therefore look for a wave function of the form^{40,43}

$$\langle \underline{z} | N, M, \underline{t} \rangle = \exp \left[m \sum_i^N \omega(z_i) \right] \langle \underline{z} | N, M \rangle, \quad (3)$$

where the function

$$\omega(z) = \sum_{k>0} \left[t_k z^k + \frac{t_{-k}}{(z - z_0)^k} \right] \quad (4)$$

is analytic inside the Corbino disk (shown in Fig. 2), and \underline{t} denotes a set of parameters t_k , $k \in \mathbb{Z}$. In Sec. II A we show that the shape of the deformed disk is given by the solution of a two-dimensional electrostatic problem, with $\omega(z)$ playing the role of an external potential.

We utilize the wave function (3) in two ways. First of all, small incompressible deformations are known to be the gapless excitations of the QH state.⁴ Therefore, in order to describe the low-energy physics, we will use the wave functions (3) to project the microscopic Hamiltonian of the MZ interferometer onto the subspace corresponding to incompressible deformations. Second, we investigate the effect a modulation gate located near one of the arms of the interferometer. If a negative potential is applied to such a gate, the 2DEG is depleted locally. In Sec. II A we show that the following choice of wave function

$$\langle \underline{z} | N, M, \Phi \rangle_G = \exp \left[\sum_i^N (\Phi/\Phi_0) \omega_G(z_i) \right] \langle \underline{z} | N, M \rangle, \quad (5)$$

with $\omega_G(z) = -\sum_{k>0} z^k/kz_U^k$, describes the local deformation of a Corbino disk near the point z_U , $|z_U| = r_U$ on its outer edge. This deformation is parameterized by the total magnetic flux Φ through the depleted region and the location, z_U , of the gate.

Finally, after the adiabatic insertion of a singular magnetic flux Φ through the hole in the Corbino disk at the point z_0 , the wave function is multiplied by the phase factor $\prod_i \exp[-i\Phi/\Phi_0 \arg(z_i - z_0)]$. At the same time, the wave function is deformed by the spectral flow in order to preserve its single-valuedness. This effect is described by the additional multiplier $\prod_i (z_i - z_0)^{\Phi/\Phi_0}$. The overall effect of a singular flux on the wave function can thus be represented by replacing the original wave function by

$$\langle \underline{z} | N, M, \Phi \rangle_F = \prod_i^N |z_i - z_0|^{\Phi/\Phi_0} \langle \underline{z} | N, M \rangle \quad (6)$$

It is important to note that the function (6) is single-valued, and it describes an incompressible deformation of the initial state (2).

A. Plasma analogy and incompressible states

The classical plasma analogy⁷ has proven to be an efficient method in the analysis of QH states.^{44,45} It relies on

the important observation that the norm of the Laughlin wave function may be written as the partition function of an ensemble of N classical particles interacting via the two-dimensional (logarithmic) Coulomb potential. In the large- N limit the evaluation of the partition function reduces to solving a two-dimensional electrostatic problem. Here we apply this method directly to the wave function (3). We write

$$Z = \int d^2 z_1 \dots d^2 z_N |\langle \underline{z} | N, M, \underline{t} \rangle|^2 = \int d^2 z_1 \dots d^2 z_N e^{-m E_{\text{pl}}}, \quad (7)$$

where the inverse temperature of the plasma is m and the energy is given by the expression:

$$E_{\text{pl}} = - \sum_{i<j} \ln |z_i - z_j|^2 + \sum_i \left[\frac{|z_i|^2}{2ml_B^2} - \sum_i \frac{M}{m} \ln |z_i - z_0|^2 - 2\text{Re} \omega(z_i) \right] \quad (8)$$

Introducing the microscopic density operator $\rho(z) = \sum_i \delta^2(z - z_i)$, we can formally write

$$E_{\text{pl}} = -\frac{1}{2} \iint d^2 z d^2 w \rho(z) \rho(w) \ln |z - w|^2 - \int d^2 z \rho(z) \varphi_{\text{ext}}(z), \quad (9)$$

where

$$\varphi_{\text{ext}}(z) = -\frac{|z|^2}{2ml_B^2} + \frac{M}{m} \ln |z - z_0|^2 + 2\text{Re} \omega(z), \quad (10)$$

and normal ordering is assumed in the first term on the right hand side of Eq. (9) in order to remove the self-interaction contribution. This representation makes it obvious, that the partition function (7) describes a gas of charged particles interacting via the 2D Coulomb potential that are confined by the external potential $\varphi_{\text{ext}}(z)$. The first term in Eq. (10) describes the interaction with a neutralizing homogeneous background charge of density $\rho_{\text{bg}} = (1/4\pi)\Delta(|z|^2/2ml_B^2) = 1/2\pi ml_B^2$. The second term can be viewed as describing a repulsion from a macroscopic charge M/m at the point z_0 . Finally, the last term describes the effect of an external (chargeless, since $\Delta \text{Re} \omega(z) = 0$) potential on the particles in the gas.

The next step is to approximate the integral over coordinates in Eq. (7) by a functional integral⁴⁶ over the density $\rho(z)$:

$$Z = \int \mathcal{D}\rho(z) e^{-m E_{\text{pl}}[\rho]}. \quad (11)$$

After this approximation, which can be justified in the large- N limit,⁴⁴ the evaluation becomes straightforward. We note that the energy of the plasma is a quadratic function of the density. Hence the average density $\langle \rho(z) \rangle =$

$Z^{-1}\langle N, M, \underline{t} | \rho(z) | N, M, \underline{t} \rangle$ is given by the solution of the saddle-point equation $\delta E_{\text{pl}} / \delta \rho(z) = 0$, which reads

$$\int d^2w \langle \rho(w) \rangle \ln |z - w|^2 + \varphi_{\text{ext}}(z) = 0. \quad (12)$$

Important consequences of this simple equation are the following ones. First, it implies that the total potential vanishes in the region where $\langle \rho(z) \rangle \neq 0$, i.e. where the 2DEG is not fully depleted. In other words, the Coulomb plasma is a “perfect metal” that completely screens the external potential φ_{ext} . Applying the Laplacian to (12), we find that $\langle \rho(z) \rangle = \rho_{\text{bg}}$, i.e., the Coulomb plasma is distributed homogeneously to screen the background charge. This confirms that the wave function (3) describes an incompressible deformation of the QH droplet. In particular, the wave function (2) describes the approximate ground state of an MZ interferometer, shown in Fig. 2. Indeed, the plasma analogy suggests that the hole in the Corbino disk is formed symmetrically around the point z_0 , where the macroscopic charge M/m is located. It serves to screen this charge, so that the total potential vanishes in the region occupied by the 2DEG. Because of perfect screening, the shape of the outer edge is, however, independent of the position of the hole and displays the symmetry of boundary conditions in the background charge distribution (see first term in Eq. (10)).

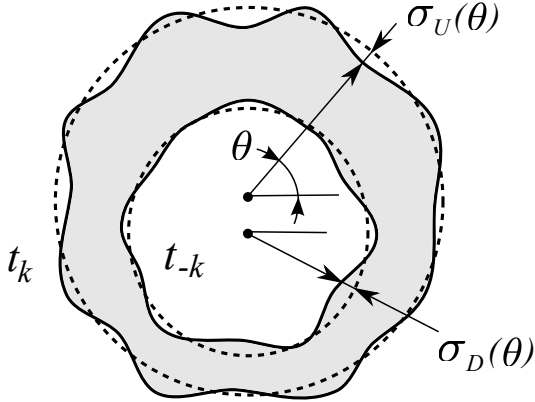


FIG. 3: A QH liquid, whose ground state is given in Eq. (3), is shown schematically. The dashed lines show the edges of the unperturbed Corbino disk, while an incompressible deformation is shown by the full lines. The region of constant electron density $\langle \rho(z) \rangle = \rho_{\text{bg}}$ is shown by the grey shadow. The shape of this region is determined by the complex function $\omega(z)$ defined in Eq. (4). The Fourier components of a charge density σ_U accumulated at the outer edge are given by the coefficients t_k of the regular part of the Laurent series for $\omega(z)$, while the Fourier components of a charge density σ_D accumulated at the inner edge are given by the coefficients t_{-k} of the singular part of $\omega(z)$ [see Eq. (14)].

We now investigate the effect of the potential $\omega(z)$ perturbatively. Let us denote by D the region to which the QH system is confined. We search for the solution of Eq. (12) in the form $\langle \rho(z) \rangle = \rho_{\text{bg}}$, for $z \in D$, and $\langle \rho(z) \rangle = 0$

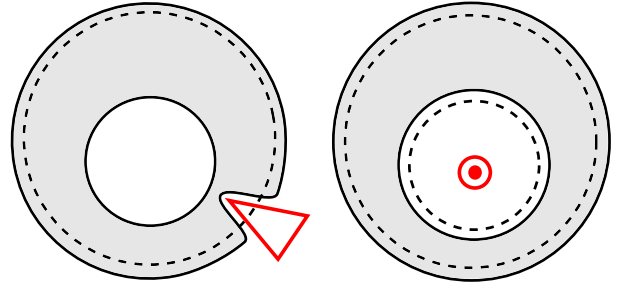


FIG. 4: The effects of a modulation gate and of a singular flux are illustrated. *Left panel:* The modulation gate locally depletes the QH liquid. Due to the incompressibility of the QH liquid, the repelled charge is accumulated homogeneously along the edge. *Right panel:* In the language of the Coulomb plasma, the multiplier in the wave function (6) depending on the singular flux can be viewed as a point-like charge placed in the center of the inner hole. It homogeneously shifts both edges to preserve the electro-neutrality.

otherwise. Thus we can rewrite Eq. (12) as

$$\rho_{\text{bg}} \int_D d^2w \ln |z - w|^2 + \varphi_{\text{ext}}(z) = 0$$

Introducing a small deformation, $D = D_0 + \delta D$, and taking into account that the integral over the undeformed Corbino disk, D_0 , cancels the first two terms in Eq. (10), we arrive at the following result

$$\rho_{\text{bg}} \int_{\delta D} d^2w \ln |z - w| + \text{Re} \omega(z) = 0 \quad (13)$$

In polar coordinates (see Fig. 3), the boundaries of the deformed disk can be parameterized as $r(\theta) = r_s + \sigma_s(\theta)/\rho_{\text{bg}}$, where $s = U, D$, and $\sigma_s(\theta)$ are the 1D charge densities accumulated at the inner and outer edge due to the deformation.

Because of perfect screening in the two-dimensional Coulomb plasma, one can solve Eq. (13) independently for each edge. Using the series expansion $\ln |z - w| = \ln |w| - \text{Re} \sum_{k>0} (z/w)^k / k$, for $|z| \leq |w|$, and the explicit expression (4) for the potential $\omega(z)$, we solve equation (13) by power series. The result can be presented in the form of Fourier series:

$$2\pi r_U \sigma_U(\theta) = 2\text{Re} \sum_{k>0} k t_k r_U^k e^{ik\theta} \quad (14a)$$

$$2\pi r_D \sigma_D(\theta) = 2\text{Re} \sum_{k>0} k t_{-k} r_D^{-k} e^{-ik\theta} \quad (14b)$$

These series show how the microscopic wave function (3) determines the shape of the deformed Corbino disk.

Finally, we analyze the effects of a modulation gate and of a singular magnetic flux, as illustrated in Fig. 4. According to the result (14), the deformation described by the wave function (5) has the following form:

$$r_U \sigma_U(\theta) = -\frac{\Phi}{m\Phi_0} \left(\delta(\theta - \theta_0) - \frac{1}{2\pi} \right), \quad (15)$$

where θ_0 is the argument of the position, z_U , of the modulation gate. This function correctly captures the effects of the modulation gate: the local depletion of the 2DEG at the point $z_U = r_U e^{i\theta_0}$ and the homogeneous expansion of the QH liquid due to its incompressibility. It is easy to check that the flux through the depleted area under the modulation gate, $-B \int (\sigma_U / \rho_{bg}) r_U d\theta$, is indeed equal to Φ . In the presence of a singular magnetic flux, the plasma energy contains an additional term

$$\delta E_{pl} = -\frac{\Phi}{m\Phi_0} \sum_i \ln |z_i - z_0|^2. \quad (16)$$

In the language of the Coulomb plasma it describes the addition of a charge $\Phi/m\Phi_0$ in the hole of the interferometer at the point z_0 . This homogeneously shifts the edges of the Corbino disk by an amount $\delta r_s = (\Phi/m\Phi_0)(1/2\pi r_s \rho_{bg})$, $s = U, D$, as illustrated in Fig. 4.

B. Low-energy subspace

Having found the set of states (3) describing incompressible deformations of a QH liquid, we proceed to construct operators generating the subspace of such low-energy states when applied to the undeformed ground-state and finding their commutation relations. First of all, let us introduce zero-mode operators changing the number of electrons N and quasi-particles M in the system

$$e^{i\phi} |N, M, \underline{t}\rangle = |N, M+1, \underline{t}\rangle \quad (17a)$$

$$e^{i\phi_N} |N, M, \underline{t}\rangle = |N+1, M, \underline{t}\rangle. \quad (17b)$$

States with different numbers of electrons N are obviously orthogonal, while the overlaps of wave functions with different numbers of quasi-particles M are strongly suppressed in the large- N limit.⁷ Taking this observation into account, one derives from the definitions (17) the following commutation relations for the operators of zero modes⁴⁷

$$[M, e^{i\phi}] = e^{i\phi}, \quad [N, e^{i\phi_N}] = e^{i\phi_N}. \quad (18)$$

Next, we introduce deformation operators a_{ks} , $s = U, D$, for any $k > 0$, acting from the right as

$$a_{kU} |N, M, \underline{t}\rangle = \sqrt{k} r_U^k t_k |N, M, \underline{t}\rangle, \quad (19a)$$

$$a_{kD} |N, M, \underline{t}\rangle = \sqrt{k} r_D^{-k} t_{-k} |N, M, \underline{t}\rangle. \quad (19b)$$

The states (3) are coherent states under the action of these operators. In order to find commutation relations for these operators, we need to evaluate scalar products of the states (3).

We start with the norm of a wave function, which is given by the square root of the partition function of the Coulomb plasma, (7) and (11), and evaluate the “free energy”

$$F_{pl} = -(1/m) \log(Z). \quad (20)$$

Considering the potential $\omega(z)$ as a perturbation, we obtain

$$F_{pl} = F_0 - \frac{\rho_{bg}^2}{2} \iint_{\delta D} d^2 z d^2 w \ln |z - w|^2,$$

where the constant F_0 is the contribution from the unperturbed state and from the determinant of the Gaussian integral. We evaluate this integral with the help of the solution (14) and present the result as a bilinear form in the coefficients t_k ,

$$F_{pl}(\underline{t}^*, \underline{t}) = F_0 - \sum_{k>0} k [r_U^{2k} t_k^* t_k + r_D^{-2k} t_{-k}^* t_{-k}] - \sum_{k \geq k' > 0} k' C_k^{k'} [z_0^{k-k'} t_k t_{-k'} + \text{c.c.}], \quad (21)$$

where $C_k^{k'}$ are binomial coefficients. The holomorphic structure of this bilinear form allows us to extend the result for the norm $Z = \exp\{-mF_{pl}(\underline{t}^*, \underline{t})\}$ to the scalar products $\langle N, M, \underline{t} | N, M, \underline{t}' \rangle = \exp\{-mF_{pl}(\underline{t}^*, \underline{t}')\}$.

Next, we define differential operators, via their matrix elements, as follows: $\langle \Psi | \partial / \partial t_k | N, M, \underline{t}' \rangle = -\partial / \partial t'_k \langle \Psi | N, M, \underline{t}' \rangle$. A straightforward calculation then yields:

$$\langle N, M, \underline{t} | \frac{\partial}{\partial t_k} | N, M, \underline{t}' \rangle = - \left[m k r_U^{2k} t_k^* + \sum_{k' \leq k} m k' C_k^{k'} z_0^{k-k'} t_{-k'}' \right] \langle N, M, \underline{t} | N, M, \underline{t}' \rangle. \quad (22)$$

Using definition (19), we may write $\langle N, M, \underline{t} | a_{kU}^\dagger | N, M, \underline{t}' \rangle \equiv \langle N, M, \underline{t}' | a_{kU} | N, M, \underline{t} \rangle^* = \sqrt{k} r_U^k t_k^* \langle N, M, \underline{t} | N, M, \underline{t}' \rangle$. Substituting this equation in (22) we finally express the adjoint operators acting on the states $|N, M, \underline{t}\rangle$, via the parameters t_k , as

$$a_{kU}^\dagger = -\frac{r_U^{-k}}{m\sqrt{k}} \left(\frac{\partial}{\partial t_k} - \sum_{k' \leq k} k' C_k^{k'} z_0^{k-k'} t_{-k'} \right). \quad (23)$$

Repeating exactly the same calculations for the operators $\partial / \partial t_{-k}$, we obtain:

$$a_{kD}^\dagger = -\frac{r_D^k}{m\sqrt{k}} \left(\frac{\partial}{\partial t_{-k}} - \sum_{k' \geq k} k C_k^{k'} z_0^{k'-k} t_{k'} \right). \quad (24)$$

Using expressions (19), (23) and (24) for the operators a_{ks} and their adjoints and the relation $[\partial / \partial t_k, t_{k'}] = \delta_{kk'}$, we obtain the commutation relations:

$$[a_{ks}, a_{k's'}^\dagger] = \frac{1}{m} \delta_{kk'} \delta_{ss'}. \quad (25)$$

Similarly, one finds that $[a_{ks}^\dagger, a_{k's'}^\dagger] = [a_{ks}, a_{k's'}] = 0$. Thus the deformation operators, a_{ks} and a_{ks}^\dagger , introduced in (19) satisfy canonical commutation relations, and the subspace of incompressible deformations has a natural Fock space structure with respect to these operators.

III. PROJECTION ONTO THE LOW-ENERGY SUBSPACE

Starting from the microscopic model, we now explicitly derive the low-energy effective theory of an interferometer. For this purpose, we project the microscopic Hamiltonian and tunneling operators of quasi-particles between the two edges onto the low-energy subspace constructed above. The projection of these operators is defined by $O \rightarrow POP$, where the orthogonal projection P is written as:

$$P = \sum_{N,M} \int \prod_k d^2 t_k \frac{1}{Z} |N, M, \underline{t}\rangle \langle N, M, \underline{t}|, \quad (26)$$

where the norm $Z = \langle M, N, \underline{t} | M, N, \underline{t} \rangle$, in the large N limit, is given by the integral (11). We first implement the projection procedure in the absence of an external magnetic flux. In Sec. III C we then consider situations where a singular flux tube is inserted and a modulation gate voltage is applied.

A. Edge Hamiltonian

The microscopic Hamiltonian for N electrons, restricted to the lowest Landau level, is given by the expression

$$H = \sum_i^N U(z_i) + \sum_{i<j}^N V(|z_i - z_j|), \quad (27)$$

where $V(|z|)$ is the potential of the screened 3D Coulomb interaction and $U(z)$ is the confining potential, which forces electrons to form the interferometer. Note that we have omitted the kinetic energy operator, since, acting on the lowest Landau level, it gives a constant contribution, $N\hbar\omega_c/2$, where $\omega_c = eB/m_e c$ is the cyclotron frequency. The projection of the microscopic Hamiltonian onto the subspace of incompressible deformations $\mathcal{H} = PHP$ is given by

$$\mathcal{H} = \sum_{N,M} \int \prod_k d^2 t_k d^2 t'_k \frac{E(\underline{t}^*, \underline{t}')}{\sqrt{ZZ'}} |N, M, \underline{t}\rangle \langle N, M, \underline{t}'|, \quad (28)$$

where $Z' = \langle N, M, \underline{t}' | N, M, \underline{t}' \rangle$, and the potential energy contribution reads

$$E(\underline{t}^*, \underline{t}') = \frac{1}{\sqrt{ZZ'}} \langle N, M, \underline{t} | H | N, M, \underline{t}' \rangle \quad (29)$$

We first consider diagonal matrix elements $E(\underline{t}^*, \underline{t})$ in (29). They can be rewritten in terms of the electronic density in the deformed state as follows:

$$E(\underline{t}^*, \underline{t}) = \int d^2 z U(z) \langle \rho(z) \rangle + \frac{1}{2} \iint d^2 z d^2 w V(|z - w|) \langle \rho(z) \rho(w) \rangle.$$

In the large- N limit and for the long-range Coulomb interaction we approximate this function as $\langle \rho(z) \rho(w) \rangle \simeq \langle \rho(z) \rangle \langle \rho(w) \rangle$, neglecting the “exchange” contribution. Thus, we may rewrite the energy of a deformation in terms of the average density as

$$E(\underline{t}^*, \underline{t}) \simeq \int d^2 z U(z) \langle \rho(z) \rangle + \frac{1}{2} \iint d^2 z d^2 w V(|z - w|) \langle \rho(z) \rangle \langle \rho(w) \rangle \quad (30)$$

Next, we propose to express the projected Hamiltonian (28) in terms of the deformation operators (19). To this end, we consider small deformations of the state (2) and take into account the fact that the density is constant, $\langle \rho(z) \rangle = \rho_{bg}$, for $z \in D$. Writing the deformed region as $D = D_0 + \delta D$, one can expand the integral (30) in the small deformation δD and evaluate the correction term with the help of the result (14):

$$E(\underline{t}^*, \underline{t}) = E_0 + m \sum_{k>0} [\varepsilon_U(k) (r_U)^{2k} k t_k^* t_k + \varepsilon_D(k) (r_D)^{-2k} k t_{-k}^* t_{-k}]. \quad (31)$$

where E_0 is the energy of a QH system confined to an undeformed Corbino disk, and the last two terms originate from the deformation δD . The excitation spectra, $\varepsilon_s(k)$, $s = U, D$, are determined by the two-body interaction and by the confining potential:

$$\varepsilon_s(k) = \frac{kU'(r_s)}{2\pi m \rho_{bg} r_s} + \frac{k}{m} \int_0^{2\pi} d\varphi V\left(2r_s \left|\sin \frac{\varphi}{2}\right|\right) [e^{ik\varphi} - e^{i\varphi}]. \quad (32)$$

Using again the holomorphic structure of the bilinear form (31) to extend this result to off-diagonal matrix elements, we arrive at the projected Hamiltonian (28) in the following form:

$$\mathcal{H} = E_0 + m \sum_{s=U,D} \sum_{k>0} \varepsilon_s(k) a_{ks}^\dagger a_{ks}. \quad (33)$$

We further assume that the potential V describes Coulomb interactions screened at a distance d . In the low-energy limit, i.e., for $kd/r_s \ll 1$, the deformation energy in (32) is then linear as a function of the mode number: $\varepsilon_s(k) \simeq v_s k/r_s$, where the constants v_s are the group velocities of edge excitations. The energy of the undeformed state takes the following form as a function of the number of electrons N and the number of quasi-particles M :

$$E_0(N, M) = \frac{v_D}{2mr_D} M^2 + \frac{v_U}{2mr_U} (M + mN)^2. \quad (34)$$

Replacing the mode number with the wave vector $k \rightarrow k/r_s$, we arrive at the final expression for the edge Hamiltonian

$$\mathcal{H} = E_0(N, M) + m \sum_{s=U,D} \sum_{k>0} v_s k a_{ks}^\dagger a_{ks} \quad (35)$$

We conclude this section with the following important remark. Equation (32) contains two terms: the first term is the drift velocity, proportional to the boundary electric field, $E(r_s)$, while the second one is proportional to the “Coulomb logarithm”

$$v_s = cE(r_s)/B + (e^2/m\hbar) \ln(d/l_B). \quad (36)$$

The ultraviolet cutoff in (36) is determined by correction terms in a $1/N$ -expansion of the two-point density correlation function. In fact, result (36) coincides with an expression proposed earlier in Ref. [29] on the basis of the classical electrostatic picture.

B. Tunneling Hamiltonian

The tunneling Hamiltonian for an MZ interferometer may be written as a sum of tunneling operators at the left and right QPC:

$$H_T = \sum_{\ell=L,R} [A(\xi_\ell) + A^\dagger(\xi_\ell)].$$

The tunneling operator is an operator annihilating a quasi-particle at a point ξ' on one edge and recreating it at a point ξ on the other edge:

$$A(\xi) = \psi_{\text{qp}}^\dagger(\xi) \psi_{\text{qp}}(\xi'), \quad (37)$$

where ψ_{qp}^\dagger and ψ_{qp} are quasi-particle operators. As for the edge Hamiltonian, the projection of the tunneling operator, $\mathcal{A} = PA(\xi)P$, is expressed in terms of matrix elements in deformed states $\langle N, M, \underline{t} | A(\xi) | N, M', \underline{t}' \rangle$. These matrix elements can be found by inserting a complete set of intermediate states:

$$\begin{aligned} \langle N, M, \underline{t} | A(\xi) | N, M', \underline{t}' \rangle &= \int \prod_i d^2 z_i \\ &\times \langle N, M, \underline{t} | \psi_{\text{qp}}^\dagger(\xi) | \underline{z} \rangle \langle \underline{z} | \psi_{\text{qp}}(\xi') | N, M', \underline{t}' \rangle \end{aligned} \quad (38)$$

In other words, we define the tunneling operator as an operator whose matrix elements are overlaps of wave functions with quasi-particles located on the inner and the outer edge.

The wave functions with insertion of a quasi-particle, $\langle \underline{z} | \psi_{\text{qp}}(\xi) | N, M, \underline{t} \rangle$ are constrained by the condition that the annihilation of m quasi-particles at the same point is equivalent to the annihilation of an electron. The electron operator is defined by $\langle z_1, \dots, z_N | \psi_{\text{el}}(\xi) | \Psi \rangle = \sqrt{N+1} \langle z_1, \dots, z_N, \xi | \Psi \rangle$, which leads to the result:

$$\begin{aligned} \langle \underline{z} | \psi_{\text{el}}(\xi) | N+1, M, \underline{t} \rangle &= (\xi - z_0)^M e^{-|\xi|^2/4l_B^2 + m\omega(\xi)} \\ &\times \prod_i (\xi - z_i)^m \langle \underline{z} | N, M, \underline{t} \rangle, \end{aligned} \quad (39)$$

where we omitted a combinatorial factor, because it can be absorbed into the tunneling amplitudes. A quasi-particle at the point ξ is therefore described by the following wave function:

$$\begin{aligned} \langle \underline{z} | \psi_{\text{qp}}(\xi) | N, M, \underline{t} \rangle &= (\xi - z_0)^{M/m} e^{-|\xi|^2/4ml_B^2 + \omega(\xi)} \\ &\times \prod_i (\xi - z_i) \langle \underline{z} | N, M, \underline{t} \rangle \end{aligned} \quad (40)$$

Expression (40) differs from Laughlin’s quasi-particle definition only by a constant factor. We show in Appendix A that the quasi-particle operator, obtained by the projection of $\psi_{\text{qp}}(\xi)$ defined by (40) onto the low-energy subspace, satisfies all the physical requirements (locality, charge and statistics).

In order to evaluate the matrix elements (38), we first assume that $\underline{t}' = \underline{t}$, as in the previous section, and then generalize our findings. The product $\prod_i (\xi - z_i)$ in Eq. (40) can be rewritten as $\exp[\sum_i \ln(\xi - z_i)]$. Thus, expanding the logarithms in power series on the outer edge, $\ln(\xi' - z_i) = \ln \xi' - \sum_{k>0} z_i^k/k\xi'^k$, and on the inner edge, $\ln(z_i - \xi) = \ln(z_i - z_0) - \sum_{k>0} (\xi - z_0)^k/k(z_i - z_0)^k$, we arrive at the following expression for the matrix elements (38):

$$\begin{aligned} \langle N, M, \underline{t} | A(\xi) | N, M', \underline{t} \rangle &= (\xi^* - z_0^*)^{M/m} (\xi - z_0)^{M'/m} \exp[-|\xi|^2/2ml_B^2 + \omega(\xi) + \omega^*(\xi^*) + N \ln \xi] \\ &\times \int \prod_i d^2 z_i (z_i^* - z_0^*)^k \exp \left\{ - \sum_{k>0} \left[\frac{z_i^k}{k\xi^k} + \frac{(\xi^* - z_0^*)^k}{k(z_i^* - z_0^*)^k} \right] \right\} \langle N, M, \underline{t} | \underline{z} \rangle \langle \underline{z} | N, M', \underline{t} \rangle. \end{aligned} \quad (41)$$

Here we have assumed for simplicity that tunneling points are close to each other and have set $\xi' = \xi$.

Taking into account that $\sum_i z_i^k \langle \underline{z} | N, M', \underline{t} \rangle = \partial/\partial t_k \langle \underline{z} | N, M', \underline{t} \rangle$ and $\sum_i (z_i^* - z_0^*)^{-k} \langle N, M, \underline{t} | \underline{z} \rangle =$

$\partial/\partial t_{-k}^* \langle N, M, \underline{t} | \underline{z} \rangle$, we pull out of the integral the power series in z_i . Then we use the fact that $\langle N, M, \underline{t} | \underline{z} \rangle \prod_i (z_i^* - z_0^*) = \langle N, M+1, \underline{t} | \underline{z} \rangle$ to rewrite the expression (41) in the following form:

$$\begin{aligned} \langle N, M, \underline{t} | A(\xi) | N, M', \underline{t} \rangle &= (\xi^* - z_0^*)^{M/m} (\xi - z_0)^{M'/m} \exp[-|\xi|^2/2ml_B^2 + \omega(\xi) + \omega^*(\xi^*) + N \ln \xi] \\ &\times \exp \left\{ - \sum_{k>0} \left[\frac{1}{k\xi^k} \frac{\partial}{\partial t_k} + \frac{(\xi^* - z_0^*)^k}{k} \frac{\partial}{\partial t_{-k}^*} \right] \right\} \langle N, M+1, \underline{t} | N, M', \underline{t} \rangle. \end{aligned} \quad (42)$$

One can immediately see that the matrix element (42) vanishes unless $M' = M + 1$.

Finally, using expression (21) for the logarithm of the norm $Z = \langle M, N, \underline{t} | N, M, \underline{t} \rangle$ and definition (19), we can write the projection of the tunneling operator (37) in terms of the deformation operators as follows:

$$\mathcal{A}(\xi) = t \cdot \exp \left[-i\phi + N \ln \xi + i\varphi_U(\xi) - i\varphi_D^\dagger(\xi^* - z_0^*) \right], \quad (43)$$

where all the constant multiplicative factors are absorbed into a prefactor t , and we have introduced the following notations:

$$\varphi_U(\xi) = i \sum_{k>0} \frac{1}{\sqrt{k}} \left[(r_U/\xi)^k a_{kU}^\dagger - (\xi/r_U)^k a_{kU} \right], \quad (44a)$$

$$\varphi_D(\xi) = i \sum_{k>0} \frac{1}{\sqrt{k}} \left[(\xi/r_D)^k a_{kD}^\dagger - (r_D/\xi)^k a_{kD} \right]. \quad (44b)$$

To complete our description of the low-energy physics of the interferometer we must find the projection of the operators of electron tunneling from the quantum Hall edges to the Ohmic contacts. This can be done by applying the technique used above to the electron annihilation operator (39). The result of the projection is given by

$$\begin{aligned} \mathcal{A}_U &= t_U c_U^\dagger \exp \left[im\varphi_U(\xi_U) \right] \\ &\times \exp \left[i\phi_N + mN \ln \xi_U + M \ln(\xi_U - z_0) \right] \end{aligned} \quad (45)$$

for tunneling from the outer edge to the upper Ohmic contact (see Fig. 2 for notations), while the tunneling operator on the inner edge is given by

$$\begin{aligned} \mathcal{A}_D &= t_D c_D^\dagger \exp \left[im\varphi_D(\xi_D - z_0) \right] \\ &\times \exp \left[i\phi_N + im\phi + M \ln(\xi_D - z_0) \right], \end{aligned} \quad (46)$$

To conclude this section we note that one can find the projected charge density operators at the edges of a QH system, $\rho_D(\theta) = P\sigma_D(\theta)P - M/2\pi mr_D$ and $\rho_U(\theta) = P\sigma_U(\theta)P + (M + mN)/2\pi mr_U$, by rewriting the result (14) directly in terms of the operators (19):

$$\rho_D(\theta) = -\frac{1}{2\pi r_D} \partial_\theta \varphi_D(\xi) - \frac{M}{2\pi m r_D}, \quad (47a)$$

$$\rho_U(\theta) = \frac{1}{2\pi r_U} \partial_\theta \varphi_U(\xi) + \frac{M + mN}{2\pi m r_U}. \quad (47b)$$

Here the homogeneous contributions describe the charge accumulation caused by the variation of quantum numbers M and N . Expressions (47) lead to the following commutation relations

$$[\mathcal{A}(\xi), \rho_s(\theta)] = \pm \frac{1}{mr_s} \delta(\theta - \theta_s) \mathcal{A}(\xi), \quad (48)$$

where the angles θ_D and θ_U parametrize the position of the tunneling point in coordinates of the inner and outer edge. These commutation relations show that the tunneling operator (43) creates a pair of point-like charges of magnitude $\pm 1/m$. Similarly, one can check that the operators (45) and (46) create a unit charge at the corresponding edge. Expressions (43-47) complete the projection procedure (see also Appendix A). The resulting low-energy theory agrees well with the effective theory of Refs. [5] and [6].

C. Effect of a singular flux and a modulation gate voltage

Having outlined a self-consistent procedure for the projection of observables onto low-energy states, we next consider the projection of the edge Hamiltonian and of the tunneling operators in the situation where a magnetic flux is threading through the interferometer. First, we consider the situation where the flux is varied by application of a modulation gate voltage. The wave function of the interferometer in this situation is given by Eq. (5), and the edge density in this state is given by Eq. (15). Similarly to Eq. (3), we define deformations of the ground state (5) as follows:

$$\begin{aligned} \langle \underline{z} | N, M, \Phi, \underline{t} \rangle_G &= \prod_i^N \exp \left[m\omega(z_i) \right. \\ &\left. + (\Phi/\Phi_0)\omega_G(z_i) \right] \langle \underline{z} | N, M \rangle, \end{aligned} \quad (49)$$

where $\omega_G(z) = -\sum_{k>0} z^k/kz_U^k$ describes the local deformation of a Corbino disk near the point z_U , $|z_U| = r_U$ on its outer edge. The scalar products of these states can be deduced from Eq. (21). They are given by the following expression:

$$\begin{aligned} \langle N, M, \Phi, \underline{t} | N, M, \Phi, \underline{t}' \rangle_G \\ = \exp \left[-mF_{\text{pl}}(t_k^* + t_{0k}^*, t_k' + t_{0k}') \right], \end{aligned} \quad (50)$$

where $t_{0k} = -(\Phi/m\Phi_0)/kz_U^k$, for $k > 0$, and $t_{0k} = 0$, for $k < 0$. Using the result (50), one concludes that the algebra of deformation operators (25) does not change after the application of a gate voltage.

Next, we find that the edge density in the state (49) coincides with the result (14), but with t_k replaced by $t_k + t_{0k}$. This does not affect the energy of small deformations, which is still bilinear in the coefficients t_k .

Therefore, the only effect of the modulation gate on the edge Hamiltonian, up to irrelevant constants, is given by:

$$E_0(N, M, \Phi) = \frac{v_D}{2mr_D} M^2 + \frac{v_U}{2mr_U} (M + mN + \Phi/\Phi_0)^2. \quad (51)$$

We can also find the projection of the tunneling operators by applying the shift $t_k \rightarrow t_k + t_{0k}$ to formula (43), which yields

$$\mathcal{A}(\xi) = t \exp[\omega_G(\xi)\Phi/m\Phi_0] \times \exp[-i\phi + N \ln \xi + i\varphi_U(\xi) - i\varphi_D^\dagger(\xi^* - z_0^*)]. \quad (52)$$

Thus, we note that, after an application of a gate voltage, the tunneling operators $\mathcal{A}(\xi_L)$ at the left QPC and $\mathcal{A}^\dagger(\xi_R)$ at the right QPC acquire a relative phase $\delta\phi = (\Phi/m\Phi_0)[\omega_G(\xi_L) + \omega_G^*(\xi_R^*)]$ proportional to the flux Φ through the region of 2DEG depleted by the modulation gate. Using the explicit form of the function $\omega_G(\xi_L)$, we arrive at the following expression:

$$\delta\phi = \frac{2\pi\Phi}{m\Phi_0} \left(1 - \frac{L_U}{2\pi r_U}\right). \quad (53)$$

where L_U is the length of the outer arm of the interferometer (see Fig. 5). We will show in Sec. V B that only the topological part $2\pi\Phi/m\Phi_0$ of this phase enters tunneling rates, while the geometry-dependent part cancels exactly with the zero-mode contribution.

The situation where the flux is changed via the insertion of a singular flux tube is described by the wave function (6). In Sec. II A we have shown that the insertion of a singular flux is equivalent to the insertion of a point-like charge (in classical plasma language) and that it leads to a homogeneous shift of the edges. Thus, we find the projected edge Hamiltonian by replacing M with $M + \Phi/\Phi_0$ (to take into account the shift of the edges), which yields

$$E_0(N, M, \Phi) = \frac{v_D}{2mr_D} (M + \Phi/\Phi_0)^2 + \frac{v_U}{2mr_U} (M + mN + \Phi/\Phi_0)^2. \quad (54)$$

The wave functions of the deformed states in the presence of a singular flux Φ differ from (3) only by the factor $\prod_i |z_i - z_0|^{\Phi/\Phi_0}$. Thus the tunneling operator can be found with the help of the same calculations as in Sec. III B, which yields an expression that differs from Eq. (43) only by a real prefactor:

$$\mathcal{A} = t|\xi - z_0|^{2\Phi/\Phi_0} \times \exp[-i\phi + N \ln \xi + i\varphi_U(\xi) - i\varphi_D^\dagger(\xi^* - z_0^*)] \quad (55)$$

We conclude that, in contrast to the situation where a modulation gate is introduced, the tunneling operators at different QPCs do not acquire any relative phases due to the singular flux. This is interpreted as an exact cancellation of the phase shift caused by the flux itself and

the phase shift caused by charge accumulation at the edges. In Sec. IV, we show that this fact is universal, i.e., it does not depend on the specific wave function (2) of the interferometer.

IV. EFFECTIVE THEORY

In this section we show that the low-energy effective theory, derived, in the last section, from the specific wave function (3), can be formulated in a universal gauge-invariant form. In order to do so, we start from the topological Chern-Simons theory^{6,41} in the bulk of a QH system and construct a boundary action so that the total action is local and gauge invariant. Then we show that the gauge-invariant edge Hamiltonian coincides with the one derived from microscopic theory, see Eq. (35), and tunneling amplitudes coincide with those given by Eq. (43). Finally, we show that the independence of the tunneling amplitudes on a singular flux is a gauge-invariant effect, caused by topological screening of a magnetic flux by the Chern-Simons field.

A. Gauge invariant action

We begin by recalling the construction of the effective low-energy theory of an infinitely extended QH liquid at filling factor $\nu = 1/m$. Such a liquid is described by a conserved current, j^μ . The continuity equation, $\partial_\mu j^\mu = 0$, is solved by introducing potentials B_μ ,

$$j^\mu = \frac{1}{2\pi} \epsilon^{\mu\nu\lambda} \partial_\nu B_\lambda. \quad (56)$$

Here and below, we use units where $e = \hbar = 1$, and adopt the Einstein summation convention, unless specified otherwise. The current is invariant under the gauge transformations $B_\mu \rightarrow B_\mu + \partial_\mu \beta$. By counting dimensions, it is easy to see that the gauge invariant action for the potential B given by

$$S[B] = \frac{m}{4\pi} \int d^3r \epsilon^{\mu\nu\lambda} B_\mu \partial_\nu B_\lambda \quad (57)$$

has zero dimension, while all other possible terms have *lower* dimensions, i.e., are *irrelevant* at large distance- and low energy scales. For example, the Maxwell-like term has dimension -1 .

Next, the interaction with an external electromagnetic field, described by a vector potential A_μ , is given by the term:

$$S_{\text{int}}[A, B] = \int d^3r A_\mu J^\mu = \frac{1}{2\pi} \int d^3r A_\mu \epsilon^{\mu\nu\lambda} \partial_\nu B_\lambda.$$

Integrating out the fields B_μ , we arrive at an effective action for the electromagnetic field in the Chern-Simons form:

$$S_{\text{eff}}[A] = \frac{1}{4\pi m} \int d^3r \epsilon^{\mu\nu\lambda} A_\mu \partial_\nu A_\lambda.$$

The average current $\langle J^\mu \rangle = \delta S_{\text{eff}}[A]/\delta A_\mu$ is then given by Hall's law:

$$\langle J^\mu \rangle = \sigma_H \epsilon^{\mu\nu\lambda} \partial_\nu A_\lambda,$$

where $\sigma_H = 1/2\pi m$ is the Hall conductivity. Thus, we conclude that, for an infinitely extended liquid, the action (57) correctly describes the QH effect at $\nu = 1/m$.

However, in the situation where a QH liquid is confined to a finite region D , the effective action for the QH liquid in the presence of an external electromagnetic field,

$$S[A, B] = \frac{1}{4\pi m} \int_D d^3r \epsilon^{\mu\nu\lambda} [2A_\mu + mB_\mu] \partial_\nu B_\lambda, \quad (58)$$

is not gauge invariant.³⁶ Namely, one easily sees that, under a gauge transformation $A_\mu \rightarrow A_\mu + \partial_\mu \alpha$, $B_\mu \rightarrow B_\mu + \partial_\mu \beta$, the action (58) transforms as $S[A, B] \rightarrow S[A, B] + \delta S[A, B]$ with:

$$\begin{aligned} \delta S[A, B] &= \frac{1}{4\pi} \int_D d^3r \epsilon^{\mu\nu\lambda} [2\partial_\mu \alpha + m\partial_\mu \beta] \partial_\nu B_\lambda \\ &= \frac{1}{4\pi} \int_{\partial D} d^2r [2\alpha + m\beta] \epsilon^{\mu\nu} \partial_\mu b_\nu \end{aligned} \quad (59)$$

where $b = B|_{\partial D}$ is the restriction of the bulk field B to the boundary ∂D . A physical reason for the gauge anomaly is the fact that in a QH liquid confined to a finite region the bulk Hall current (56) is not conserved. Consequently, the electric charge may accumulate at the edge of the sample.

In order to restore the gauge invariance of the effective theory, we take into account the boundary degrees of freedom. It is easy to see that the boundary action

$$S[\phi] = \frac{m}{4\pi} \int_{\partial D} d^2r [D_t \phi D_x \phi - h(D_x \phi) + \epsilon^{\mu\nu} b_\mu \partial_\nu \phi], \quad (60)$$

which is similar to the action found in Ref. [36] from a quantization of the hydrodynamics of a charged liquid, cancels the gauge anomaly (59), provided one assumes that the edge field ϕ transforms as

$$\phi \rightarrow \phi - (2/m)\alpha - \beta, \quad (61)$$

and the covariant derivative is given by the expression

$$D_\mu \phi = \partial_\mu \phi + (2/m)a_\mu + b_\mu.$$

Note that the commutation relations for the field $\phi(x)$ are determined by the first term in the canonical action (60):

$$[\partial_x \phi(x), \phi(y)] = \frac{2\pi i}{m} \delta(x - y). \quad (62)$$

However, the precise form of the boundary Hamiltonian density $h(D_x \phi)$ is not fixed by the effective theory. The only requirement is that the Hamiltonian density should

be a positive definite function of $D_x \phi$. The simplest possible expression $h = v(D_x \phi)^2$, justified in the case of small edge deformations, leads to the chiral edge dynamics with a linear dispersion law.

Finally, the expression for the charge density at the edge of a QH system may be found by evaluating the derivative $\rho = -\delta S/\delta a_t$ of the total action with respect to the boundary field. The result reads:

$$\rho = \frac{1}{2\pi} D_x \phi \quad (63)$$

Note that, after integrating out the fields B_μ , the action constructed above leads, for a trivial topology, to the effective theory that has been considered in Ref. [36].

B. Quasi-particle tunneling operators: Comparison with microscopic calculations

Having constructed a gauge invariant low-energy action for an incompressible QH liquid, we proceed to analyze the spectrum of local excitations. The action (57) arises in the context of a topological field theory, where excitations are described by Wilson lines.⁴¹ For instance, a general local excitation at the point r may be written as:

$$\psi_q(r) = \exp\left(iq \int^r dr^\mu B_\mu\right), \quad (64)$$

where q is a constant. The statistical phase of two excitations of the type (64) is determined by braiding the corresponding Wilson lines.⁴¹ Considering two excitations labeled by q_1 and q_2 , one arrives, after a simple calculation of braiding, at the following expression for the statistical phase: $\theta_{12} = \pi q_1 q_2 / m$. Moreover, if one defines the charge operator as an integral over a space-like plane $Q_{\text{em}} = (1/2\pi) \int d^2r \epsilon^{\nu\lambda} \partial_\nu B_\lambda$, then the charge of the excitation (64) is given by $Q_{\text{em}} = q/m$. The above expressions for the statistical phase and the charge show that the excitation (64) with $q = m$ has the quantum numbers of an electron, while for $q = 1$ in (64) this operator has the quantum numbers of a Laughlin quasi-particle.

An operator that creates a Laughlin quasi-particle at the point ξ and a Laughlin quasi-hole at the point ξ' has the form of a Wilson line between these points:

$$\psi^\dagger(\xi) \psi(\xi') = \exp\left(i \int_\xi^{\xi'} dr^\mu B_\mu\right). \quad (65)$$

Note, however, that this operator is not gauge invariant. According to the gauge transformation of edge fields, Eq. (61), the *gauge-invariant* operator of tunneling between two edge states, described by the fields ϕ_U and ϕ_D correspondingly,⁴⁸ may be written as

$$\mathcal{A}(\xi) = t \cdot e^{i\phi_U(x)} \exp\left(i \int_\xi^{\xi'} dr^\mu \left[B_\mu + \frac{2}{m} A_\mu\right]\right) e^{-i\phi_D(x)}, \quad (66)$$

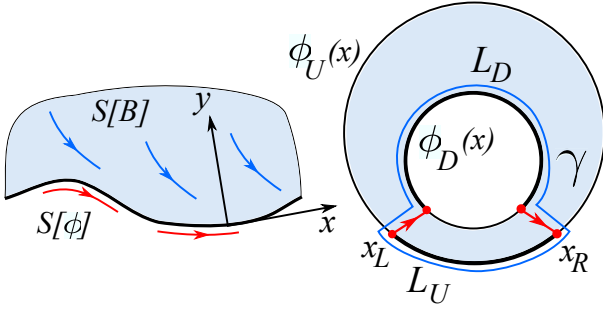


FIG. 5: Illustration of the model of a MZ interferometer based on the gauge-invariant effective theory of a QH liquid. *Left panel:* The QH liquid, shown in gray shadow, is bounded to a finite region with an edge shown by a thick black line. The bulk current (blue arrows) is not conserved at the edge. The corresponding anomaly inflow is canceled by an edge current (red arrows), which is described by the action (60). For the edge degrees of freedom, we chose the coordinates so that the x -axis is tangential to the edge. *Right panel:* An MZ interferometer has two edges which are described by the fields $\phi_U(x)$ (outer edge) and $\phi_D(x)$ (inner edge). The operators of tunneling at QPCs, located at points x_L and x_R , are given by the Wilson lines (shown in red) joining pairs of points on opposite edges. The phase of the product (73) of two such operators contains two contributions: One contribution arises from the integral of the bulk fields over the interference contour γ (blue line), and the other one comes from the charge accumulated at the arms of the interferometer (thick lines). The length of the inner arm is denoted by L_D , while the length of the outer arm is L_U .

where the 1D and 2D coordinates are related via the expression $\xi' = r_U e^{ix/r_U}$ for the outer edge and $\xi - z_0 = r_D e^{ix/r_D}$ for the inner edge of the MZ interferometer; (see Fig. 5). The tunneling operator (66) creates a pair of local charges of the value $1/m$ at the edges, which may be checked by evaluation of the commutator of this operator with the charge density operator (63) with the help of Eq. (62).

To compare the tunneling operator (66) with the microscopic one, Eq. (43), we first note that, assuming the tunneling path is short, one may set $\xi = \xi'$ and neglect the Wilson line contribution in Eq. (66). Next, we introduce a normal mode expansion for the edge densities ρ_s , $s = U, D$:

$$2\pi\rho_D(x) = -\frac{M}{mr_D} + \sum_{k>0} \sqrt{\frac{k}{r_D}} [a_{kD} e^{-ikx} + \text{h.c.}], \quad (67a)$$

$$2\pi\rho_U(x) = \frac{M + mN}{mr_U} + \sum_{k>0} \sqrt{\frac{k}{r_U}} [a_{kU} e^{ikx} + \text{h.c.}], \quad (67b)$$

where the summation ranges over the wave vector k . Here the operators a_{ks} and a_{ks}^\dagger obey the canonical commutation relations (25). This guarantees that the commutation relation (62) is satisfied, when zero modes are taken

into account. Moreover, the edge Hamiltonian

$$\mathcal{H} = \pi m \int dx [v_U \rho_U^2(x) + v_D \rho_D^2(x)], \quad (68)$$

expressed in terms of the operators a_{ks} and a_{ks}^\dagger , coincides with the microscopically derived Hamiltonian (35).

Finally, in this section and later in this paper, the fields ϕ_s naturally contain zero-mode contributions.⁴⁹ In order to find these contributions we need to know the vacuum distribution of the field B_μ at the edges for a state with given values of zero modes M and N . This field describes the homogeneous distribution of the QH liquid in the interferometer and thus satisfies the equation $\epsilon^{\mu\nu} \langle \partial_\mu B_\nu \rangle = 2\pi\rho_{\text{bg}}$. Typically, for a fixed geometry, one subtracts the background contribution from the Chern-Simons field and sets $\langle B_\mu \rangle = 0$. However, in the present case of a Corbino disk geometry, the field $\langle B_\mu \rangle$ varies, depending on the numbers M and N . We find the field by taking into account the change in the background charge ρ_{bg} caused by the variation of the quantum numbers M and N . To this end, we note that the field $\epsilon^{\mu\nu} \langle B_\nu \rangle$ may be viewed as an “electric field” that satisfies Gauss’ law with the constant charge density ρ_{bg} . The variation of the number M leads to a shift of the edges of the Corbino disk, and to an accumulation of a background charge $\pm M$ in the form of two homogeneous rings. Solving the 2D electrostatic problem we find that $\langle B_\mu \rangle = 0$ on the inner edge and

$$\langle B_\mu \rangle = M \partial_\mu [\arg(\xi) - \arg(\xi - z_0)] \quad (69)$$

on the outer one.

We use the distribution (69), the normal mode expansion (67), and the relation (63) between the edge densities and edge fields to arrive at the following expressions

$$\begin{aligned} \phi_U &= \phi_N/m + Nx/r_U + (M/m) \arg(r_U e^{ix/r_U} - z_0) \\ &\quad + i \sum_{k>0} [a_{kU}^\dagger e^{-ikx} - \text{h.c.}] / \sqrt{kr_U}, \end{aligned} \quad (70a)$$

$$\begin{aligned} \phi_D &= \phi + \phi_N/m + Mx/mr_D \\ &\quad + i \sum_{k>0} [a_{kD}^\dagger e^{ikx} - \text{h.c.}] / \sqrt{kr_D}, \end{aligned} \quad (70b)$$

which should be compared to Eq. (44). We conclude that the tunneling operator (66), in the absence of an external electromagnetic field A_μ , coincides with the microscopic expression (43) if one sets $\xi = \xi'$. It is important to note that the contributions of zero modes to the edge fields are strongly affected by the specific geometry of an MZ interferometer. Namely, the phase shift of the tunneling amplitude caused by the zero mode M is not constant along the outer edge, provided $z_0 \neq 0$.

C. Effect of a singular flux and a modulation gate voltage

In this section we show that the effects of a singular flux and of a modulation gate found in Sec. III C can be

reformulated in terms of the gauge-invariant low-energy effective theory. We start from the situation where the modulation gate voltage is applied in order to deform the outer edge of a MZ interferometer. This situation can be described at the level of the effective theory by adding a term in the Hamiltonian, that describes the interaction of the potential φ_{mg} created by the modulation gate with charge density accumulated at the edge. Thus, the total Hamiltonian of the outer edge is given by the expression:

$$\mathcal{H}_U = \int dx [\pi m v_U \rho_U^2(x) + \varphi_{\text{mg}}(x) \rho_U(x)].$$

Then we find the ground-state expectation value of the charge density by minimizing the Hamiltonian with the constraint $\int dx \rho_U(x) = 0$.

For the situation where the gate is located at the point x_0 , we approximate the potential as $\varphi_{\text{mg}}(x) = \alpha \delta(x - x_0)$. The expectation value of the density is then given by

$$\delta \rho_U(x) = -\frac{\alpha}{2\pi m v_U} \left[\delta(x - x_0) - \frac{1}{2\pi r_U} \right].$$

The parameter α can be expressed in terms of the flux Φ through the region depleted by the gate, $\alpha = 2\pi v_U \Phi / \Phi_0$, so that the expression for the accumulated charge density acquires the form

$$\delta \rho_U(x) = -\frac{\Phi}{m \Phi_0} \left[\delta(x - x_0) - \frac{1}{2\pi r_U} \right]. \quad (71)$$

Finally, we redefine the charge density on the outer edge by subtracting the vacuum contribution (71): $\rho_U \rightarrow \rho_U + \delta \rho_U$. As a consequence, the edge Hamiltonian (68) acquires an additional term:

$$\mathcal{H} = \pi m \int dx \left[v_D \rho_D^2(x) + v_U \left(\rho_U(x) + \frac{1}{2\pi r_U} \frac{\Phi}{m \Phi_0} \right)^2 \right]. \quad (72)$$

Substituting into this equation the normal mode expansion (70), we arrive at the result (35) with the vacuum energy E_0 given by Eq. (51), in full agreement with the microscopic theory.

Next, we investigate the effect of the modulation gate on the tunneling operator (66). We will show in the next section that, to lowest order in the tunneling Hamiltonian, the AB contribution to the current is determined by the product of two such operators taken at two QPCs. Therefore, only a relative phase of the tunneling operators has a physical meaning. We express this product in terms of the edge densities with the help of Eq. (63):

$$\begin{aligned} \mathcal{A}(\xi_L) \mathcal{A}^\dagger(\xi_R) &\propto \exp \left(i \int_\gamma dr^\mu \left[B_\mu + \frac{2}{m} A_\mu \right] \right) \\ &\times \exp \left(-2\pi i \int_{x_L}^{x_R} dx [\rho_U(x) + \rho_D(x)] \right). \end{aligned} \quad (73)$$

Here γ is the interference contour, x_ℓ , $\ell = L, R$ are positions of the QPCs, and the integral of densities extends over the arms of the interferometer (see Fig. 5).

Then, as explained above, we subtract the vacuum charge density (71) accumulated due to the interaction with the modulation gate. The product (73) of tunneling operators then acquires a phase shift $\delta\phi = -2\pi \int_{x_L}^{x_R} dx \delta \rho_U(x)$. Using the explicit expression for $\delta \rho_U$ in the situation where the gate is located at a point x_0 between the QPCs, we arrive at the result (53). Thus, we see that calculations based on the gauge-invariant effective theory fully agree with the microscopic derivation of the tunneling operators.

It remains to investigate the effect of a singular magnetic flux. To this end, we minimize the action (60) with respect to the edge densities in the presence of an external electromagnetic field. This leads to the following equations of motion:

$$\partial_t \rho_s - v_s \partial_x \rho_s = \frac{1}{2\pi m} E_x, \quad (74)$$

where $s = U, D$, and E_x is the component of the electric field along the edge of the sample. It follows from this equation that, in equilibrium, $\partial_t \rho_s = 0$, and for $E_x = 0$, the accumulated charges are always homogeneously distributed along the edges: $\partial_x \rho_s = 0$. Moreover, integrating Eq. (74) over the coordinate x and subtracting the equation for the inner edge ($s = D$) from the equation for the outer one ($s = U$), we arrive at the following equation:

$$\partial_t M = \frac{\partial_t \Phi}{\Phi_0}, \quad (75)$$

where Φ is the flux through the interferometer. Here we have used Maxwell's equations and restored physical units. Thus, we conclude that, after the adiabatic insertion of the singular flux, the quantum number M is shifted by Φ/Φ_0 . This, in turn, leads to an effective Hamiltonian of the form:

$$\mathcal{H} = \pi m \sum_{s=U,D} \int dx v_s \left[\rho_s(x) + \frac{1}{2\pi r_s} \frac{\Phi}{m \Phi_0} \right]^2.$$

Using again the normal mode expansion (70), we arrive at the Hamiltonian (35), with the vacuum energy E_0 given by Eq. (54), in agreement with the microscopic theory.

Finally, one can see from the expansion (70) that the tunneling operator (66) for $\xi \simeq \xi'$ does not depend on M . Therefore, it does not change after the insertion of the singular flux. This effect may be interpreted as an exact cancellation of two contributions to the phase of expression (73). The first contribution arises from the gauge-invariant integral $\int_\gamma dr^\mu [B_\mu + (2/m)A_\mu]$ of the bulk fields over the interference contour γ upon variation of the singular flux. The second one is proportional to the charge $\int dx [\delta \rho_U(x) + \delta \rho_D(x)]$ accumulated along the arms of the interferometer. Physically, this means that the phase shift of an edge excitation along a closed contour γ caused directly by a variation of the vector potential A_μ is screened by the phase shift caused by the concomitant reconstruction of the QH liquid. This kind

of *topological* screening is the reflection, on the effective-theory level, of the fact that after the insertion of the singular flux the microscopic wave function (6) undergoes a deformation in order to preserve its single-valuedness.

V. INTERFEROMETER OUT OF EQUILIBRIUM

We have shown above that the AB effect, in its original formulation, does not exist in QH interferometers, because the tunneling operators do not depend on the singular magnetic flux threading the Corbino disk. This, however, does not imply that the current through the interferometer is independent of the flux. In this section we demonstrate that it oscillates as a function of Φ with the electronic period Φ_0 , in agreement with the Byers-Yang theorem. These oscillations originate from the Coulomb blockade effect and hence vanish in the thermodynamic limit⁵⁰ and in the limit of strong coupling to Ohmic contacts. In contrast, oscillations of the current as a function of the modulation gate voltage originate from quantum interference. Therefore they do not vanish in the thermodynamic limit.

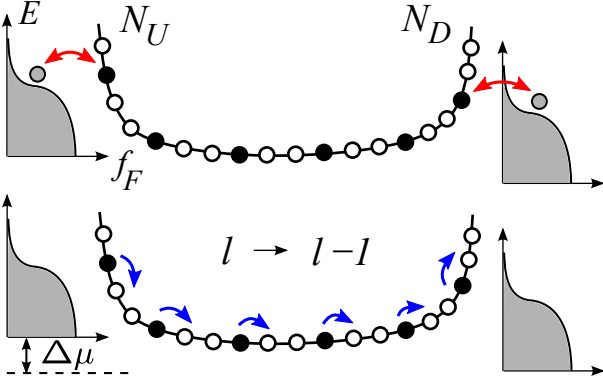


FIG. 6: Schematic illustration of the processes at Ohmic contacts and QPCs. *Upper panel:* Electrons tunnel between Ohmic contacts and QH edges, preserving the incompressibility of the QH liquid. These processes change the numbers N_U and N_D . *Lower panel:* Tunneling of a quasi-particle from one edge of the Corbino disk to another leads to the reconstruction of the wave function and changes the number l by 1. It is accompanied by a change of the electric charge at the inner edge by the value $1/m$.

We consider a MZ interferometer, strongly coupled to Ohmic contacts, with weak quasi-particle tunneling between inner and outer edge (see Fig. 6). The strong coupling of electrons to Ohmic contacts guarantees that the inner and outer edge states are in equilibrium with the metallic reservoirs, with corresponding electro-chemical potentials μ_U and μ_D . The charge current between Ohmic contacts, arising as a response to the potential difference $\Delta\mu = \mu_U - \mu_D$, is due to weak quasi-particle tunneling at the QPCs. It is then convenient to introduce a new notation for zero modes. We denote by N_U

and N_D the numbers of electrons at the outer and inner edge of the interferometer, respectively. The number of quasi-particles localized on the inner edge is denoted by $l = 0, \dots, m-1$:

$$M = mN_D - l, \quad (76)$$

$$M + mN = mN_U - l. \quad (77)$$

The electron quantum numbers, N_U and N_D , change due to tunneling at the Ohmic contacts while the quantum number l changes by 1 when a quasi-particle tunnels from one edge to the other one, as illustrated in Fig. 6.

Without loss of generality, we consider the zero modes to be classical variables and derive a master equation for the probability distribution functions. Quantum coherence manifests itself in oscillations of the quasi-particle tunneling rates as functions of the magnetic flux Φ . These oscillations originate from the interference of the two quasi-particle tunneling amplitudes at the left and right QPC. Formally, these oscillations stem from the Φ -dependent phase factor in the tunneling operators.

A. Master equation and tunneling rates

In this section we derive the master equation that describes weak quasi-particle tunneling, and we find the tunneling rates using the effective theory constructed above. The strong coupling to Ohmic contacts implies that, after every event of quasi-particle tunneling, the edge states relax to the equilibrium state described by the probability distribution function

$$P_l(N_U, N_D) = \frac{1}{Z_l} e^{-\beta(E_0 - \sum_s \mu_s N_s)}, \quad (78)$$

where β is the inverse temperature, μ_s is the electrochemical potential of the s^{th} Ohmic contact, and Z_l is the partition function. The probability $P_l(N_U, N_D)$ depends on the number l of quasi-particles via the ground-state energy $E_0(N_U, N_D, l)$, given by Eq. (34). Importantly, one does not need to specify the precise form of coupling to the Ohmic contacts, because the only role of this coupling is to equilibrate the edge states.⁵¹

To lowest order in quasi-particle tunneling, the full distribution function of zero modes may be written as

$$P(N_U, N_D, l) = \mathcal{P}_l P_l(N_U, N_D), \quad (79)$$

where \mathcal{P}_l is the probability to find the system in a state with l quasi-particles, and $P_l(N_U, N_D)$ plays the role of a conditional probability to find the interferometer in a state with N_U and N_D electrons at the edges, for a given number l of quasi-particles.

Considering quasi-particle tunneling as a weak process that changes the number l , we may describe it with the master equation

$$\dot{\mathcal{P}}_l = \Omega_{l-1}^+ \mathcal{P}_{l-1} + \Omega_{l+1}^- \mathcal{P}_{l+1} - (\Omega_l^+ + \Omega_l^-) \mathcal{P}_l, \quad (80)$$

where Ω_l^+ and Ω_l^- are the rates of transition from the state with l quasi-particles to the state with $l+1$ and $l-1$ quasi-particles, respectively. These rates are given by the expression:

$$\Omega_l^\pm = \sum_{N_U, N_D} W_l^\pm(N_U, N_D) P_l(N_U, N_D), \quad (81)$$

where $W_l^\pm(N_U, N_D)$ are the rates of quasi-particle tunneling between two states with fixed numbers of electrons, N_U and N_D .

At time scales much larger than the characteristic times of tunneling, the interferometer reaches a steady state regime with $\dot{P}_l = 0$. It is easy to see that in this regime the following quantity is independent of l

$$I = \Omega_l^+ P_l - \Omega_{l+1}^- P_{l+1}. \quad (82)$$

This quantity is in fact the charge current that we are looking for. This follows from the expression for the current

$$I = (1/m) \sum_l (\Omega_l^+ - \Omega_l^-) P_l, \quad (83)$$

and from the periodic boundary condition, $P_0 = P_m$, which can be verified directly using equations (78) and (79). Note that the detailed balance equation $\Omega_l^+ P_l = \Omega_{l+1}^- P_{l+1}$ is satisfied only if $I = 0$. Thus, the MZ interferometer in a non-equilibrium steady-state regime represents an interesting example of a system with broken detailed balance.

We evaluate the tunneling rates $W_l^\pm(N_U, N_D)$ to leading order in the tunneling Hamiltonian $\mathcal{H}_T = \mathcal{A} + \mathcal{A}^\dagger$, where $\mathcal{A} \equiv \mathcal{A}(\xi_L) + \mathcal{A}(\xi_R)$. A straightforward calculation, based on the Fermi Golden Rule, gives the following expression:

$$W_l^+(N_U, N_D) = \int dt \text{Tr} \{ \rho_{\text{eq}} \mathbb{P}(N_U, N_D, l) \mathcal{A}^\dagger(t) \mathcal{A}(0) \}, \quad (84)$$

and a similar expression for $W_l^-(N_U, N_D)$. Here the operator $\mathbb{P}(N_U, N_D, l)$ projects onto states with given numbers N_s and l , and the operator ρ_{eq} is the equilibrium density matrix for the oscillators.

Next, we outline some further steps, the details of which may be found in Refs. [29] and [36]. We write the equations of motion for the tunneling operators $\mathcal{A}(\xi_\ell)$, $\ell = L, R$, by evaluating the commutator of the operator (43) with the Hamiltonian (35), and solve these equations in order to find the time evolution of \mathcal{A} . As a result, we arrive at the following expression for the tunneling rates taking the form of a sum of an incoherent and coherent part:

$$W_l^\pm(N_U, N_D) = \int dt e^{i\Delta E_\pm t} \left[(|t_L|^2 + |t_R|^2) \prod_s K_s(t) + \text{Re } t_L t_R^* e^{iN \ln(\xi_L \xi_R^*)} \prod_s K_s(t - L_s/v_s) \right], \quad (85)$$

Here $\Delta E_\pm(N_U, N_D, l) = E_0(N_U, N_D, l \pm 1) - E_0(N_U, N_D, l)$ is the energy difference between final states with $l \pm 1$ quasi-particles and an initial state with l quasi-particles, and the functions $K_s(t) = (\beta v_s/\pi) [\sinh(\pi t/\beta)]^{1/m}$, $s = U, D$, are the equilibrium correlation functions of the oscillator modes. We recall that $N = N_U - N_D$ is the total number of electrons in the Corbino disk, and ξ_L and ξ_R are the 2D coordinates of the QPCs. Note that the magnetic flux enters the tunneling rates (85), in particular, via the energy difference ΔE_\pm . In the next two sections we use Eqs. (51) and (54) for the energy E_0 in order to investigate the flux dependence of the tunneling rates in different situations.

B. Effect of a modulation gate: Quasi-particle AB periodicity

In the case where the flux through the interferometer is varied with the help of a modulation gate we use Eq. (51) to evaluate the energy difference between the final and initial state:

$$\Delta E_\pm = \sum_{s=U,D} \frac{v_s}{mr_s} \left(\frac{1}{2} \pm l \mp mN_s \right) \mp \frac{v_U \Phi}{mr_U \Phi_0}. \quad (86)$$

In this situation, an additional flux dependence is due to the tunneling operators $\mathcal{A}(\xi_L)$ and $\mathcal{A}(\xi_R)$ at the left and right QPCs, which acquire a relative phase $\delta\phi$ given by Eq. (53), which, for convenience, we rewrite here: $\delta\phi = (2\pi\Phi/m\Phi_0)[1 - (L_U/2\pi r_U)]$. This phase enters the interference term of the tunneling rates (85).

Next, we note that in the thermodynamic limit⁵⁰ the sum over the electronic numbers in Eq. (85) and in the expression for the partition function Z_l can be well approximated by an integral, so that we arrive at the expressions

$$\Omega_l^\pm = \frac{1}{Z_l} \int dN_U dN_D e^{-\beta(E_0 - \sum_s \mu_s N_s)} W_l^\pm(N_U, N_D). \quad (87)$$

It is convenient to shift the integration variables: $N_U \rightarrow N_U + l/m - \Phi/\Phi_0$ and $N_D \rightarrow N_D + l/m$. Important consequence of this transformation are the following ones: First of all, the energy of zero modes simplifies, $E_0 = \sum_s m v_s N_s^2 / 2r_s$, where $s = U, D$. Second, the energy difference becomes independent of the number l and of the flux: $\Delta E_\pm = \sum_s (v_s/mr_s)(1/2 \pm mN_s)$. Finally, the AB phase difference (53) takes a topological value, $\delta\phi = 2\pi\Phi/m\Phi_0$, because its geometry-dependent part cancels exactly with the contribution from the phase $N \ln(\xi_L \xi_R^*)$ in the interference term of the rates (85).

Using the new expressions for E_0 , ΔE_\pm , and $\delta\phi$, we find that the integral (87) is Gaussian with the saddle point located, in the thermodynamic limit, at

$$N_D = \frac{\mu_D r_D}{m v_D}, \quad N_U = \frac{\mu_U r_U}{m v_U}. \quad (88)$$

Substituting this values into Eq. (81), we obtain the following expressions for tunneling rates:

$$\Omega_l^\pm(\Phi) = \int dt e^{\pm(i/m)\Delta\mu t} \left[(|t_L|^2 + |t_R|^2) \prod_s K_s(t) + \text{Re } t_L t_R^* e^{2\pi i \Phi / m \Phi_0} e^{iN \ln(\xi_L \xi_R^*)} \prod_s K_s\left(t - \frac{L_s}{v_s}\right) \right], \quad (89)$$

with $N = N_U - N_D$ in the second term given by

$$N = \mu_D \frac{r_D}{mv_D} - \mu_U \frac{r_U}{mv_U}, \quad (90)$$

as follows from the expressions (88).

Thus, we arrive at a first important conclusion: The rates do not depend on l , $\Omega_l^\pm = \Omega^\pm$. This implies, according to Eq. (83), that the current is equal to $I = (1/m)(\Omega^+ - \Omega^-)$, i.e., it coincides with the expression for the current obtained in Ref. [36]. We therefore do not evaluate the integral in (89) and refer the reader to [36], where the current has been thoroughly analyzed in the linear and non-linear regimes. Second, we note that the rates (89) depend on the magnetic flux. Thus we conclude, that the AB effect survives in the thermodynamic limit if the flux is varied with the help of a modulation gate. One can see that the current has the *quasi-particle* periodicity. This result does *not* violate the Byers-Yang theorem, because the flux through the interferometer caused by the application of a modulation gate cannot be gauged away.

Finally, we note that tunneling rates (89) depend not only on the voltage bias $\Delta\mu$, but also on μ_U and μ_D separately, via the total number of electrons in the interferometer, $N = N_U - N_D$, which is given by expression (90). This seems to violate the gauge invariance. In fact, this is not the case, because we assumed, for simplicity, that the Coulomb interaction is screened by a nearby metallic gate, so that the inner and outer edges of the Corbino disk do not interact. This situation is realized in a number of recent experiments, e.g., in Ref. [24]. The additional metallic gate plays a role of the third electrode, which independently controls the number of electrons in the system. The potentials μ_U and μ_D are then measured with respect to this gate. We have to admit that the degree of screening depends on details of an experimental situation. We stress, however, that these details do not affect the generality of our conclusions concerning the periodicity of the AB oscillations.

C. Effect of a singular magnetic flux: Restoration of the electronic periodicity

Here we show that, in the situation where the flux through the interferometer is varied by inserting a singular flux tube, the electronic periodicity of the current is restored. In this case the energy difference between the

states with $l \pm 1$ and l quasi-particles is given by

$$\Delta E_l^\pm = \sum_s \frac{v_s}{mr_s} \left[\frac{1}{2} \pm \left(l - mN_s - \frac{\Phi}{\Phi_0} \right) \right]. \quad (91)$$

We may now pass to the thermodynamic limit and replace the sum over N_s by an integral to arrive at expression (87). It is then easy to see that, in the present case, after shifting variables, $N_s \rightarrow N_s + l/m - \Phi/m\Phi_0$, the integral becomes independent of the flux Φ . This is because, here, the magnetic flux enters the tunneling rates (85) only via the energy of zero modes, E_0 , in contrast to the situation where the flux is varied with the help of a modulation gate. We conclude that there is no AB effect associated with a singular flux, and in order to find the flux dependence of the tunneling rates we need to take into account terms that are small in the thermodynamic limit.

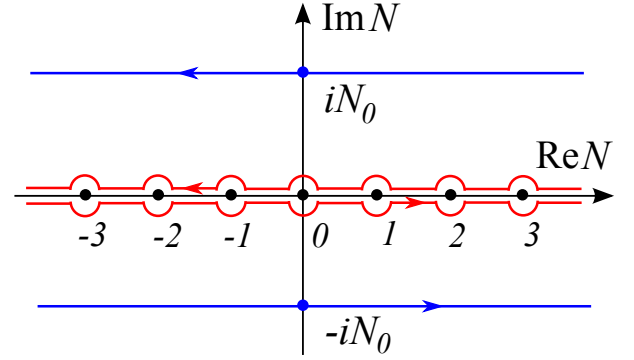


FIG. 7: Illustration of the analytical structure of the integral (92). On one hand, this integral can be presented as a sum of residues at integer points on the real axis. On the other hand, the initial integration contour, shown in red, may be deformed to a new position, shown in blue, parallel to the real axis at a distance $N_0 \gg 1$ from it.

To this end, we use an identity⁵² that allows to rewrite a sum over integer numbers as an integral,

$$\sum_N (\dots) = \frac{1}{2i} \oint dN \cot(\pi N) (\dots),$$

along the contour shown as a red line in Fig. 7. Using this identity and performing the shift of variables $N_s \rightarrow N_s + l/m + \Phi/m\Phi_0$, we arrive at the following expression for transition rates:

$$\Omega_l^\pm = \frac{1}{Z_l} \oint \prod_s dN_s \cot \pi \left(N_s + \frac{l}{m} - \frac{\Phi}{m\Phi_0} \right) \times \exp \left(-\beta m v_s N_s^2 / 2r_s + \beta \mu_s N_s \right) W_l^\pm(N_U, N_D), \quad (92)$$

where we have omitted unimportant constants, and $W_l^\pm(N_U, N_D)$ are the tunneling rates (85). We stress that after the shift of variables indicated above, the tunneling rates $W_l^\pm(N_U, N_D)$ are seen *not* to depend on the number l and the flux Φ .

Next, we use the analyticity of the rates W_l^\pm as functions of the variables N_U and N_D to deform the integration contour in (92) to the new position, $N_s = x_s \pm iN_0$, as shown in Fig. 7. Assuming that N_0 is large, we expand the cotangent in the integral (92) and keep the leading harmonic:

$$\begin{aligned} & \cot \pi \left(N_s + \frac{l}{m} - \frac{\Phi}{m\Phi_0} \right) \\ &= \mp i \mp 2ie^{-2\pi N_0} \exp \left[\pm 2\pi i \left(x_s + \frac{l}{m} - \frac{\Phi}{m\Phi_0} \right) \right]. \end{aligned}$$

Substituting this expansion into Eq. (92), we find that the first term reproduces our earlier result for the leading order contribution in the thermodynamic limit. For the second, sub-leading, term, the saddle point is located far from the real axis:

$$N_s = \frac{\mu_s r_s}{mv_s} \pm \frac{2\pi i r_s}{m\beta v_s}, \quad (93)$$

because $r_s/\beta v_s \gg 1$. This justifies the expansion of the cotangent in the thermodynamic limit.

Using the saddle point values of N_s we arrive at the following expression for the tunneling rates (81):

$$\begin{aligned} \Omega_l^\pm &= \Omega^\pm(0) + \text{Re} \sum_s f_s^\pm \exp[-2\pi^2 r_s/m\beta v_s] \\ &\times \exp \left[2\pi i \left(\frac{\mu_s r_s}{mv_s} + \frac{l}{m} - \frac{\Phi}{m\Phi_0} \right) \right], \quad (94) \end{aligned}$$

where the first term, $\Omega^\pm(0)$, is the rate (89) taken at $\Phi = 0$, and the functions f_s^\pm of μ_U and μ_D are given by expressions similar to those in Eq. (89). These functions, the exact form of which is not important, are independent of l . As expected, the tunneling rates (94) contain oscillatory contributions in Φ that are exponentially suppressed in the thermodynamic limit.⁵⁰ These oscillations may be interpreted as resulting from the Coulomb blockade effect.

Finally, we note that the flux enters the transition rates (94) solely in the combination $l - \Phi/\Phi_0$. A shift of the flux Φ by one flux quantum Φ_0 may be then compensated by the shift $l \rightarrow l + 1$. The quasi-particle current is given by expression (83), where the probabilities satisfy Eqs. (82) with the constraint $\sum_l \mathcal{P}_l = 1$. All these equations are periodic in l with period equal to m and invariant under the replacement $\Omega_l^\pm \rightarrow \Omega_{l+1}^\pm$. This implies that the average current has the electronic periodicity, $I(\Delta\mu, \Phi) = I(\Delta\mu, \Phi + \Phi_0)$, in agreement with the Byers-Yang theorem. For example, the solution of Eqs. (82) and (83) for $\nu = 1/3$ gives the average current

$$I = \frac{\Omega_2^+ \Omega_1^+ \Omega_0^+ - \Omega_2^- \Omega_1^- \Omega_0^-}{\sum_l (\Omega_{l+1}^+ \Omega_l^+ + \Omega_{l+1}^- \Omega_l^- + \Omega_{l+1}^- \Omega_l^-)}, \quad (95)$$

which is explicitly periodic function of Φ with the electronic period Φ_0 . At the same time, each tunneling rate

Ω_l^\pm has a quasi-particle periodicity. Therefore, the quasi-particle periodicity with respect to a singular flux may in principle be observed via, e.g., the current noise measurements at finite frequencies. The last fact does not violate the Byers-Yang theorem, because this theorem applies only to a stationary state and to long-time measurements.

VI. DISCUSSION

The effect of topological screening plays a central role in resolving the Byers-Yang paradox. We have shown, both on the microscopic and on the effective theory levels, that it leads to a cancellation of the total AB phase due to the singular magnetic flux tube threading through the interferometer's loop and of the phase shift accumulated as a result of the physical displacement of the state. It is this last fact that makes interferometers based on QH systems to stand out from the variety of other electronic interferometers, where the AB effect is regarded nowadays as a simple textbook physics. We then conclude that the AB effect, in its original formulation, does not exist in QH interferometers. To further illuminate an important role of topological screening, we will consider here a simple example of a QH liquid at filling factor $\nu = 1$, where our theory also applies.

According to a commonly used single-particle picture, electrons in $\nu = 1$ state drift along the equipotential lines. One may then consider a QH interferometer to be an open system, where single-particle orbits form a loop as shown in the upper panel of Fig. 1, and apply the scattering theory. Since the position of the orbits does not change, being fixed by the equipotential lines, the only effect of the singular magnetic flux is to shift the phase of single-particle wave functions, which leads to the overall AB phase shift $\delta\phi = 2\pi\Phi/\Phi_0$ in scattering amplitudes. Finally, using the Landauer-Büttiker formula,⁵³ one easily finds that the average current should oscillate as a function of the singular flux with the period Φ_0 , in strong contradiction with the effect of topological screening.

Addressing this problem, we first reiterate that (i) the QH effect has a topological character, therefore the naive open systems approach may not be applicable to QH interferometers, and (ii) topological screening stems from the cooperative action of many electrons, so that the single-particle picture may not correctly describe the effect of insertion of the singular flux. As we demonstrate below, the single-particle picture is consistent with the microscopic description of the $\nu = 1$ state, particularly with the many-particle Laughlin wave function (1), only in the case of an axially symmetric Corbino disk (i.e., for $z_0 = 0$). However, in this case the AB phase shift cancels locally with the phase shift caused by the physical displacement of the orbits after the insertion of the singular flux, in full agreement with the effect of topological screening. One may argue, though, that a realistic interferometer is not symmetric: it is a small part of a larger

QH system. Therefore, we will focus now on the case of an asymmetric Corbino disk (see Fig. 8) and show that the single-particle description violates the Pauli principle.

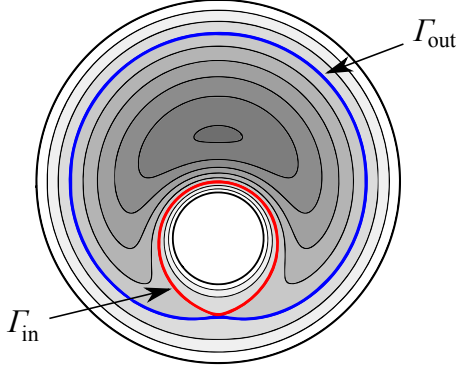


FIG. 8: The shape of an asymmetric Corbino disk is determined by the confining potential, shown here by the level of the gray shadow. The equipotential lines are shown by thin black lines. The eigenstates of a free Hamiltonian, moving along the equipotential lines, belong to three groups: those located inside the separatrix Γ_{in} , between Γ_{in} and Γ_{out} , and outside the separatrix Γ_{out} . Orbits of the first and of the third group encircle the hole of the disk, therefore they move upon the adiabatic insertion of the singular flux. The orbits between the lines Γ_{in} and Γ_{out} are not affected by the flux. This leads to the accumulation or a depletion of the density along the lines Γ_{in} and Γ_{out} .

Indeed, in a QH system, the eigenstates of the non-interacting Hamiltonian are the single-particle orbits that drift along the equipotential lines, shown in Fig. 8 as thin black lines. Two separatrices (blue line Γ_{out} and red line Γ_{in}) split the orbits into three groups with different angular momenta with respect to the hole in the Corbino disk, i.e., with respect to $z = z_0$. Initially, in a ground state all the single-particle orbits inside the Corbino disk are filled. The adiabatic insertion of the singular flux through the hole at the point z_0 does not affect the orbits between two separatrices, because those orbits do not encircle the flux. At the same time, the orbits that belong to the other two groups encircle the flux, and therefore, shift inwards or outwards in order to maintain single valuedness. This leads to the accumulation or depletion of the charge density in the regions along the lines Γ_{out} and Γ_{in} . Thus we conclude that the single-particle picture, based on the eigenstates of a non-interacting Hamiltonian, fails to correctly describe the insertion of the singular flux, because it leads to compressible deformations in the bulk of the 2DEG.

The correct approach consists of using the single-particle basis which corresponds to unconfined orbits $\psi_k = z^k \exp(-|z|^2/4l_B^2)$. These are not the eigenstates of a non-interacting Hamiltonian in the presence of a confining potential. Nevertheless, before the insertion of the singular flux two bases are equivalent to each other and related by a unitary transformation. After the insertion

of the flux, the correct single-particle basis leads to the wave function (6), which describes *incompressible* deformations.

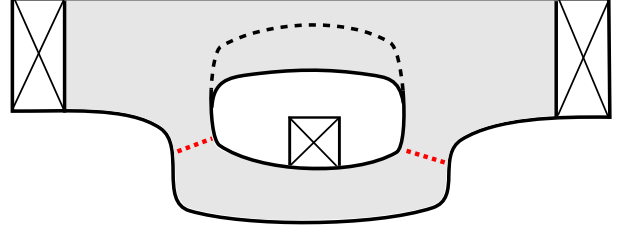


FIG. 9: Schematic of an experimental setup that may be used to detect the effect of topological screening. The 2DEG is confined to the region shown by gray shadow. Additional gate allows to partially deplete the 2DEG so that it becomes confined to the new region, shifted as shown by the dashed line. The total area enclosed by the interferometer becomes larger after the application of the gate voltage. However, due to the effect of topological screening only the flux through the QH liquid contributes to the AB phase, and it remains unchanged.

In the end, we would like to mention that the insertion of a singular flux is an idealization introduced in this paper in order to formulate the effect of topological screening. Such a procedure is not easily realizable in experiment. Therefore, in what follows we consider some physical consequences of the effect of topological screening in QH systems where a homogeneous magnetic field is varied. We note that even in this case the total magnetic flux through the hole in the MZ interferometer is screened and gives no contribution to the AB phase, because the homogeneous flux may be viewed as a distributed singular flux. This screening effect can, in principle, be tested in an experiment with a MZ interferometer at filling factor $\nu = 1$. Namely, one should apply a voltage to an additional gate in order to significantly change the size of the hole in the interferometer, without affecting the total area of the QH liquid enclosed by the interfering paths, as shown in Fig. 9. We predict that due to the effect of topological screening the period of AB oscillations as a function of the homogeneous magnetic field will remain unchanged, despite the strong variation of the geometrical area of the interferometer after the application of the gate voltage.

Next, we consider the effect of topological screening in QH systems with a long-range disorder. If the filling factor is slightly different from the value $\nu = 1/m$, but the QH system is still at the corresponding plateau of the Hall conductivity, then there are several unoccupied localized states in the bulk. This implies, that the incompressible QH liquid in the bulk of the 2DEG contains several holes, which result from the fluctuations of the disorder potential. Due to the effect of topological screening, the flux through these holes does not contribute to the AB phase. Therefore, the AB phase is proportional only to the total area of the incompressible QH liquid in the

interferometer $S_{\text{eff}} = \nu S$, and not to the geometrical area S . This should lead to a linear dependence of the period of AB oscillations on the magnetic field:

$$\Delta B = \Phi_0 / \nu S \propto B. \quad (96)$$

In addition, in samples with a strong disorder, so that the fluctuating potential exceeds the cyclotron gap, such a behavior should be present in a range of magnetic fields that is larger than the width of a single plateau. We think that the linear magnetic field dependence (96) might have already been observed in a number of experiments on Fabry-Pérot interferometers.^{16,54}

VII. CONCLUSION

Recently, the physics of AB oscillations in electronic interferometers has become a subject of a debate. A number of works have claimed that only the electronic periodicity may be observed in MZ interferometers based on QH states at fractional filling factors $\nu = 1/m$. We have briefly reviewed those papers in the introduction, and in more detail, in the Appendix C of our earlier paper [36]. Here we recall that the main argument against the observability of AB oscillations with a longer, quasi-particle periods is based on the Byers-Yang theorem, which states that the steady-state current through the interferometer oscillates with the electronic period Φ_0 as a function of the singular magnetic flux Φ threading through the interferometer's loop. Different proposed models have in common that they do not differentiate between three methods of the variation of the flux, namely, by inserting the singular flux tube, by applying a modulation gate voltage, and by varying a homogeneous magnetic field. All these models rely on the effective theory approach.

In our earlier paper we have criticized those works and argued that the average current may oscillate with the quasi-particle period $m\Phi_0$ in response to the modulation gate voltage, and yet this behavior does not violate the Byers-Yang theorem (see Appendix C of Ref. [36]). However, the arguments based solely on the effective theory seem to be insufficient. Therefore, in the present paper we refine our approach and justify it on the microscopic, effective, and kinetic theory levels. We consider the Laughlin variational wave function of the $\nu = 1/m$ state, which is known to have extremely large overlap with the exact wave function, and construct the space of gapless incompressible deformations of the QH liquid of the MZ interferometer. We proceed by projecting the microscopic Hamiltonian on the subspace of such excitations and arrive at the low-energy theory of the interferometer in the presence of a singular magnetic flux, or in the case of the applied modulation gate voltage. We derive the effective theory for a MZ interferometer from the Chern-Simons theory and find essentially perfect agreement with the results of the low-energy projection. Finally, using the effective theory, we develop the kinetic theory approach to a MZ interferometer in a

non-equilibrium current-carrying state, and find AB oscillations in the average current. We confirm that the model of Ref. [36] is correct. Our results are summarized below.

First of all, we predict the effect of topological screening of a magnetic flux threading through a hole in an incompressible QH liquid, which manifest itself in the cancellation of the total AB phase of the wave function due to the flux and of the phase shift accumulated as a result of the physical displacement of the wave function. On the microscopic level, this effect appears naturally as a consequence of the single-valuedness of the Laughlin wave function. On the effective theory level, it arises as a cancellation of the vector potential associated with the magnetic flux and of the Chern-Simons field induced by the reconstruction of the wave function in response to the insertion of the flux tube. This effect has a global, topological character, because it does not depend on the choice of the gauge. As a result, the AB effect, in its original formulation, cannot be observed in QH systems in principle. Taking into account this situation is crucial for resolving the Byers-Yang paradox.

Nevertheless, a QH system in general, and an electronic MZ interferometer in particular, will respond to the insertion of the singular flux in the form of periodic oscillations in the average steady-state current. These oscillations result from the redistribution of the charge between edge states, and from the charge quantization. However, these oscillations are associated with the Coulomb blockade effect, should have an electronic period Φ_0 , and will vanish in the thermodynamic limit, where the MZ interferometer may be considered an open quantum system. Thereby, our theory conforms to the Byers-Yang theorem. On the other hand, we predict that when the total magnetic flux Φ through the interferometer's loop is varied with the help of a modulation gate attached to one arm of the interferometer, the average current will oscillate as a function of this flux with the quasi-particle period $m\Phi_0$. Such a striking difference between two behaviors may be interpreted as if the modulation gate only “couples” to the local quasi-particle charge e/m at the edge of a QH system, while the singular flux “couples” to the global charge of Laughlin quasi-particles, which is equal to zero.

We admit that to fully resolve the controversy concerning the nature of the quasi-particle interference it is important to experimentally confirm or disprove AB oscillations with quasi-particle periods in electronic MZ interferometers. However, we understand that this experiment, which has to be done at fractional filling factors, might be not an easy task. Therefore, we suggest, as an intermediate step, to directly demonstrate the effect of topological screening by carrying out specific measurements, as explained in Sec. VI (see Fig. 9). Importantly, by doing such measurements one may observe the effect of topological screening even at integer filling factors, e.g., at $\nu = 1$. We further predict that in strongly disordered QH systems, as a result of topological screening,

the period of AB oscillations should linearly depend on the magnetic field across the plateau of the Hall conductivity.

Our additional remarks concern the properties of quasi-particle operators and of the tunneling Hamiltonians. First we note that we directly construct quasi-particle operators by projecting quasi-particle excitations of the Laughlin wave function onto the low-energy subspace. We then demonstrate that so constructed operators have anyonic commutation relations and create local excitations of the charge e/m . However, our calculations show that it is incorrect to consider such excitations as free particles propagating from one Ohmic contact to another and carrying a “statistical phase tube”. Instead, they are created by tunneling perturbations locally at QPCs. It is convenient to represent tunneling operators in term of Wilson lines, which connect end points of the tunneling paths. Then it becomes clear why tunneling operators are insensitive to the number M of quasi-particles localized at the hole of the Corbino disk, contrary to what some earlier papers suggest. This is because two Wilson lines that describe tunneling at two QPCs may be exchanged without winding the hole of the Corbino disk. Finally, we find no evidence of Klein factors in tunneling operators. Therefore, taken at two spatial points, they do not generally commute, except for a Fabry-Pérot interferometer, as explained in the Appendix A.

We conclude by saying that the proposed effective theory of an electronic MZ interferometer can be generalized to states with other filling factors than $\nu = 1/m$, in particular, to the states with non-Abelian statistics of excitations. Moreover, our results are easily generalizable to systems with a different geometry, e.g., to electronic Fabry-Pérot interferometers. Although, the physics in general will remain the same, detailed considerations may bring new interesting results. In view of our new findings concerning the nature of the quasi-particle interference, it is very interesting to reconsider the effects of quasi-particle exchange and statistics.

Acknowledgments

We thank C. W. J. Beenakker, V. Cheianov, and A. Koroliuk for valuable discussions. This work has been supported by the Swiss National Science Foundation.

Appendix A: Commutation relations for quasi-particle operators

Here we discuss commutation relations for quasi-particle operators and for tunneling operators (43) at spatially separated points. First of all, we show that the microscopic theory proposed in Sec. III leads to typical anyonic commutation relations⁵⁵ for the quasi-particle operators. To this end, we apply the projection procedure

(26) to the quasi-particle operator (40) and carry out calculations similar to those that lead to the expression (43) for tunneling operators. This procedure gives us the following expressions for the low-energy projection of quasi-particle operators

$$\begin{aligned} \psi_U(\xi) &= \exp[i\varphi_U(\xi)] \\ &\times \exp i[\phi_N/m + M/m \ln(\xi - z_0) + N \ln \xi], \end{aligned} \quad (\text{A1a})$$

$$\begin{aligned} \psi_D(\xi) &= \exp[i\varphi_D(\xi - z_0)] \\ &\times \exp i[\phi + \phi_N/m + M/m \ln(\xi - z_0)], \end{aligned} \quad (\text{A1b})$$

where the fields $\varphi_s(\xi)$ are given by Eqs. (44).

Note, that the operator (40) has zero charge, i.e., it creates a local excitation with the charge e/m together with the homogeneous density along the edge with total charge $-e/m$. Therefore, after the low-energy projection we have multiplied the quasi-particle operators by the factor $e^{i\phi_N/m}$ in order to cancel the contribution of the homogeneous density. Thus, the resulting operators (A1) indeed create local excitations with the charge e/m . Comparing equations (70) and (A1), we see that so defined fields agree with those derived in Sec. IV at the effective theory level.

Using the expressions (A1) and commutation relations (18) and (25) one easily arrives at the following relations for quasi-particle operators at the same edge:

$$\psi_U(\xi_L)\psi_U(\xi_R) = e^{\frac{i\pi}{m}\text{sign}(x_L - x_R)}\psi_U(\xi_R)\psi_U(\xi_L), \quad (\text{A2a})$$

$$\psi_D(\xi_L)\psi_D(\xi_R) = e^{\frac{i\pi}{m}\text{sign}(x_R - x_L)}\psi_D(\xi_R)\psi_D(\xi_L), \quad (\text{A2b})$$

and to similar expressions for the adjoint operators. Here we define $\xi_\ell = r_U e^{ix_\ell/r_U}$ with $\ell = L, R$ at the outer edge, and $\xi_\ell = z_0 + r_D e^{ix_\ell/r_D}$ at the inner edge. The commutation relations (A2) show that quasi-particles (A1) are anyons⁵⁵ with the statistical phase π/m .

Note, that the phase factors on the right hand side of the expressions (A2) are m -valued functions on a circle. This is consistent with the fact that quasi-particle operators are also multi-valued. Interestingly, straightforward calculations show that the operators at the opposite edges do not commute:

$$\begin{aligned} \psi_U(\xi_L)\psi_D(\xi_R) &= e^{\frac{1}{m}\arg(\xi_L - z_0) - \frac{1}{m}\arg(\xi_L)} \\ &\times \psi_D(\xi_R)\psi_U(\xi_L) \end{aligned} \quad (\text{A3})$$

In other words, a quasi-particle on the outer edge feels the presence of another quasi-particle on the inner edge. This is because the creation of a quasi-particle on the inner edge shifts quantum numbers N and M . The change of this number is a *topological* effect which leads to a reconstruction of the wave function and changes the Chern-Simons field (69).

Next, we focus on the commutation relations for the operators of quasi-particle tunneling. First of all, we would like to emphasize that at the microscopical level two tunneling operators do commute, as they are just

polynomials. However, being projected onto low-energy subspace, they do not necessary commute, if taken at different spatial points. The direct calculation for the operators (43) with the help of Eqs. (18) and (25) leads to the following expression:

$$\mathcal{A}(\xi_L)\mathcal{A}(\xi_R) = \exp\left[\frac{i}{m}\left(2\pi - \frac{L_U}{r_U} - \frac{L_D}{r_D}\right)\right]\mathcal{A}(\xi_R)\mathcal{A}(\xi_L) \quad (\text{A4})$$

In the thermodynamic limit, $r_s \rightarrow \infty$, which describes an open MZ interferometer, this leads to a simpler expression:

$$\mathcal{A}(\xi_L)\mathcal{A}(\xi_R) = e^{2\pi i/m}\mathcal{A}(\xi_R)\mathcal{A}(\xi_L), \quad (\text{A5})$$

where the statistical phase takes the topological value. For a Fabry-Pérot interferometer, setting $L_U \simeq 2\pi r_U$ and $L_D/r_D \ll 1$ and vice versa (see Fig. 5), we find

that tunneling operators commute $[\mathcal{A}(\xi_L), \mathcal{A}(\xi_R)] = 0$. We stress that the contribution of the commutator of zero modes is crucial in the above calculations. The zero modes in part related to the bulk Chern-Simons field (see the discussion at the end of Sec. IV B) and naturally take into account the topology of the interferometer.

Finally, we note that the results (A2) and (A5) provide a microscopic justification of the model of the MZ interferometer that we proposed in Ref. [36]. We have argued there that tunneling operators, derived from the effective theory of the QH edge states, do not need to commute, because the presence of a gap in the spectrum of bulk excitations of the incompressible QH liquid makes them nonlocal. Importantly, we do not see any evidence of the Klein factors³⁸ in tunneling operators (43), when expressed in terms of the quasi-particle operators (A1).

-
- ¹ K. v. Klitzing, G. Dorda, and M. Pepper, Phys. Rev. Lett. **45**, 494 (1980).
 - ² S. Datta, *Electronic transport in mesoscopic systems* (Cambridge University Press, Cambridge, 1999).
 - ³ L. D. Landau, E. M. Lifshitz, *Quantum Mechanics: Non-relativistic Theory* (Pergamon Press, 1999).
 - ⁴ *The Quantum Hall Effect*, edited by R.E. Prange and S.M. Girvin (Springer, New York, 1987).
 - ⁵ X.-G. Wen, Phys. Rev. B **41**, 12838 (1990).
 - ⁶ J. Fröhlich, A. Zee, Nucl. Phys. B **364**, 517 (1991); J. Fröhlich and T. Kerler, Nucl. Phys. B **354**, 369 (1991).
 - ⁷ R.B. Laughlin, Phys. Rev. Lett. **50**, 1395 (1983).
 - ⁸ L. Saminadayar, D.C. Glatli, Y. Jin and B. Etienne, Phys. Rev. Lett. **79**, 2526 (1997); R. de-Picciotto, M. Reznikov, M. Heiblum, V. Umansky, G. Bunin, and D. Mahalu, Nature, **389**, 162 (1997).
 - ⁹ Very recently, unexpected values of quasi-particle charges, determined via shot noise measurements, have been reported in M. Dolev, Y. Gross, Y. C. Chung, M. Heiblum, V. Umansky, and D. Mahalu, arXiv:0911.3023. These results may indicate that the Fano factor of a weak backscattering current is not determined solely by the quasi-particle charge.
 - ¹⁰ Ya. M. Blanter, and M. Büttiker, Phys. Rep. **336**, 1 (2000).
 - ¹¹ I. Safi and H. J. Schulz, Phys. Rev. B **52**, 17040 (1995).
 - ¹² H. Steinberg, G. Barak, A. Yacoby, L. N. Pfeiffer, K. W. West, B. I. Halperin, and K. Le Hur, Nature Physics **4**, 116 (2008).
 - ¹³ The use of the term “charge fractionalization” in this context is somewhat unfortunate, because, in contrast to the quasi-particle fractionalization, the corresponding process is completely classical in nature. In fact, it is very similar to the displacement current in electrical circuits.
 - ¹⁴ W. Ehrenberg, R. E. Siday, Proc. Phys. Soc. B **62**, 8 (1949); Y. Aharonov and D. Bohm, Phys. Rev. **115**, 485 (1959).
 - ¹⁵ J. A. Simmons, H. P. Wei, L. W. Engel, D. C. Tsui, and M. Shayegan, Phys. Rev. Lett. **63**, 1731 (1989); J. A. Simmons, S. W. Hwang, D. C. Tsui, H. P. Wei, L. W. Engel, and M. Shayegan, Phys. Rev. B **44**, 12933 (1991);
 - ¹⁶ F. E. Camino, W. Zhou and V.J. Goldman, Phys. Rev. Lett. **95**, 246802 (2005);
 - ¹⁷ F. E. Camino, W. Zhou and V.J. Goldman, Phys. Rev. B **72**, 075342 (2005); F. E. Camino, W. Zhou and V.J. Goldman, Phys. Rev. Lett. **98**, 076805 (2007); F. E. Camino, W. Zhou and V.J. Goldman, Phys. Rev. B **74**, 115301 (2006); R. L. Willett, L. N. Pfeiffer, K. W. West, PNAS **106**, 8853 (2009); R. L. Willett, L. N. Pfeiffer, K. W. West, arXiv:0911.0345.
 - ¹⁸ P. A. Lee, Phys. Rev. Lett. **65**, 2206 (1990); B. Rosenow, and B. I. Halperin, Phys. Rev. Lett. **98**, 106801 (2007).
 - ¹⁹ N. Byers, and C. N. Yang, Phys. Rev. Lett. **7**, 46 (1961).
 - ²⁰ Y. Ji, Y. Chung, D. Sprinzak, M. Heiblum, D. Mahalu, and H. Shtrikman, Nature (London) **422**, 415 (2003).
 - ²¹ I. Neder, M. Heiblum, Y. Levinson, D. Mahalu, and V. Umansky, Phys. Rev. Lett. **96**, 016804 (2006); I. Neder, F. Marquardt, M. Heiblum, D. Mahalu, and V. Umansky, Nature Physics **3**, 534 (2007);
 - ²² E. Bieri, *Correlation and Interference Experiments with Edge States*, PhD thesis, University of Basel (Oct. 2007); E. Bieri, M. Weiss, O. Goktas, M. Hauser, C. Schonenberger, and S. Oberholzer, Phys. Rev. B **79**, 245324 (2009);
 - ²³ P. Roulleau, F. Portier, D.C. Glatli, P. Roche, A. Cavanna, G. Faini, U. Gennser, and D. Mailly, Phys. Rev. B **76**, 161309(R) (2007); P. Roulleau, F. Portier, D.C. Glatli, P. Roche, A. Cavanna, G. Faini, U. Gennser, and D. Mailly, Phys. Rev. Lett. **100**, 126802 (2008);
 - ²⁴ L.V. Litvin, H.-P. Tranitz, W. Wegscheider, and C. Strunk, Phys. Rev. B **75**, 033315 (2007); L.V. Litvin, A. Helzel, H.-P. Tranitz, W. Wegscheider, and C. Strunk, Phys. Rev. B **78**, 075303 (2008).
 - ²⁵ E.V. Sukhorukov and V.V. Cheianov, Phys. Rev. Lett. **99**, 156801 (2007).
 - ²⁶ J.T. Chalker, Y. Gefen, and M.Y. Veillette, Phys. Rev. B **76**, 085320 (2007).
 - ²⁷ I. Neder and E. Ginossar, Phys. Rev. Lett. **100**, 196806 (2008).
 - ²⁸ S.-C. Youn, H.-W. Lee, and H.-S. Sim, Phys. Rev. Lett. **100**, 196807 (2008).
 - ²⁹ I.P. Levkivskyi and E.V. Sukhorukov, Phys. Rev. B **78**,

- 045322 (2008).
- ³⁰ D. L. Kovrizhin, and J. T. Chalker, Phys. Rev. B **81**, 155318 (2010).
- ³¹ D. J. Thouless and Y. Gefen, Phys. Rev. Lett. **66**, 806, (1991); Y. Gefen, and D. J. Thouless, Phys. Rev. B **47**, 10423, (1993).
- ³² C.L. Kane, Phys. Rev. Lett. **90**, 226802 (2003).
- ³³ K.T. Law, D. E. Feldman and Y. Gefen, Phys. Rev. B **74**, 045319 (2006).
- ³⁴ D. E. Feldman and A. Kitaev, Phys. Rev. Lett. **97**, 186803 (2006); D. E. Feldman, Y. Gefen, A. Kitaev, K. T. Law, and A. Stern, Phys. Rev. B **76**, 085333 (2007).
- ³⁵ V.V. Ponomarenko, D.V. Averin, Phys. Rev. Lett. **99**, 66803 (2007).
- ³⁶ I.P. Levkivskiy, A. Boyarsky, J. Fröhlich, E.V. Sukhorukov, Phys. Rev. B **80**, 045319 (2009).
- ³⁷ In fact, we do not agree with the idea that the average values of physical observables are determined solely by the energy spectrum of a system.
- ³⁸ R. Guyon, P. Devillard, T. Martin and I. Safi, Phys. Rev. B **65**, 153304 (2002).
- ³⁹ J.K. Jain, *Composite Fermions* (Cambridge University Press, Cambridge, 2007).
- ⁴⁰ A. Boyarsky, V.V. Cheianov, O. Ruchayskiy, Phys. Rev. B **70**, 235309 (2004).
- ⁴¹ For a review, see M. Marino, *Chern-Simons Theory, Matrix Models, and Topological Strings* (Oxford University Press, Oxford, 2005).
- ⁴² F.D.M. Haldane, E.H. Rezayi, Phys. Rev. Lett. **54**, 237 (1985); F.D.M. Haldane, in Ref. [4], Chap. 8.
- ⁴³ J. Fröhlich, *The Fractional QHE, CS Theory, and Integral Lattices*, in: Proc. of ICM'94, S.D. Chatteji (ed.), Basel, Boston, Berlin: Birkhäuser Verlag (1995).
- ⁴⁴ A. Cappelli, C.A. Trugenberger, and G.R. Zemba, Phys. Lett. B **306**, 100 (1993).
- ⁴⁵ B. Blok, X.G. Wen, Phys. Rev. B **43**, 8337 (1991); I. Kogan, A.M. Perelomov and G.W. Semenoff, Phys. Rev. B **45**, 12084 (1992); V. Gurarie, C. Nayak, Nucl. Phys. B **506**, 685 (1997); R. de Gail, N. Regnault, and M. O. Goerbig, Phys. Rev. B **77**, 165310 (2008).
- ⁴⁶ Note that the functional integration in Eq. (11) over $\rho(z)$ is constrained to the domain $\rho(z) \geq 0$.
- ⁴⁷ To be precise, the operators (17) are not unitary if N and M are finite. However, in the thermodynamic limit ($N, M \rightarrow \infty$) these operators become unitary and satisfy the commutation relations (18).
- ⁴⁸ Note that the states at the inner and outer edge have opposite chiralities. At the same time, we choose the coordinate x to run counter-clockwise at the both edges. This leads to the opposite signs of the commutators (62) of fields ϕ_U and ϕ_D , and to different signs in the expressions for edge densities ρ_U and ρ_D in terms of these fields, as e.g., in Eqs. (47).
- ⁴⁹ The zero modes (ϕ , ϕ_N , M and N in our notations) and the oscillator modes are usually treated separately in the literature on the QH edge theory (see, e.g., Ref. [26]). Here we follow our previous works^{29,36} and combine them in a single-field operator, because this simplifies the commutation relations and the edge Hamiltonian.
- ⁵⁰ The notion of the thermodynamic limit for a MZ interferometer requires some clarification. Indeed, this type of interferometers are typically considered to be open quantum systems, as illustrated in the upper panel of Fig. 1. In reality, however, electronic MZ interferometers based on a QH liquid are finite size systems. This is because they are connected to an Ohmic contact, located inside the interferometer (see the lower panel of Fig. 1). Nevertheless, it is reasonable to assume that the coupling of a MZ interferometer to Ohmic contacts is strong. Therefore, unless specified otherwise, we model this situation by taking the limit $r_s/\beta v_s \gg 1$, where $s = U, D$, i.e., assuming that the level spacing at the both edges is small compared to temperature.
- ⁵¹ One may check that solving the detailed balance equation with tunneling rates calculated with the amplitudes (45) and (46) leads to the distribution (78).
- ⁵² P. M. Morse, H. Feshbach, *Methods of theoretical physics* (New York, McGraw-Hill, 1953).
- ⁵³ R. Landauer, Philos. Mag. **21**, 863 (1970); M. Büttiker, Phys. Rev. Lett. **57**, 1761 (1986).
- ⁵⁴ F.E. Camino, Wei Zhou, V.J. Goldman, Phys. Rev. B **76**, 155305 (2007); Wei Zhou, F.E. Camino, V.J. Goldman, Phys. Rev. B **73**, 245322 (2006).
- ⁵⁵ E. Fradkin, *Field Theories of Condensed Matter Systems* (Addison-Wesley, Redwood City, 1991).